

ACCEPTED MANUSCRIPT • OPEN ACCESS

Data quality up to the third observing run of Advanced LIGO: Gravity Spy glitch classifications

To cite this article before publication: Jane Glanzer *et al* 2023 *Class. Quantum Grav.* in press <https://doi.org/10.1088/1361-6382/acb633>

Manuscript version: Accepted Manuscript

Accepted Manuscript is “the version of the article accepted for publication including all changes made as a result of the peer review process, and which may also include the addition to the article by IOP Publishing of a header, an article ID, a cover sheet and/or an ‘Accepted Manuscript’ watermark, but excluding any other editing, typesetting or other changes made by IOP Publishing and/or its licensors”

This Accepted Manuscript is © 2023 The Author(s). Published by IOP Publishing Ltd.

As the Version of Record of this article is going to be / has been published on a gold open access basis under a CC BY 3.0 licence, this Accepted Manuscript is available for reuse under a CC BY 3.0 licence immediately.

Everyone is permitted to use all or part of the original content in this article, provided that they adhere to all the terms of the licence <https://creativecommons.org/licenses/by/3.0>

Although reasonable endeavours have been taken to obtain all necessary permissions from third parties to include their copyrighted content within this article, their full citation and copyright line may not be present in this Accepted Manuscript version. Before using any content from this article, please refer to the Version of Record on IOPscience once published for full citation and copyright details, as permissions may be required. All third party content is fully copyright protected and is not published on a gold open access basis under a CC BY licence, unless that is specifically stated in the figure caption in the Version of Record.

View the [article online](#) for updates and enhancements.

9 10 Data quality up to the third observing run of 11 Advanced LIGO: Gravity Spy glitch classifications 12

14 J Glanzer¹, S Banagiri², S B Coughlin^{2,3}, S Soni⁴, M Zevin^{5,6},
15 C P L Berry^{7,2}, O Patane⁸, S Bahaadini⁹, N Rohani¹⁰,
16 K Crowston¹¹, V Kalogera², C Østerlund¹¹, L Trouille¹²,
17 A Katsaggelos^{13,2}

19 ¹Department of Physics, Louisiana State University, 202 Nicholson Hall Baton
20 Rouge, LA 70803 USA

22 ²Center for Interdisciplinary Exploration and Research in Astrophysics (CIERA),
23 Department of Physics and Astronomy, Northwestern University, 1800 Sherman Ave,
24 Evanston, IL 60201, USA

25 ³Northwestern University Information Technology Research Computing Services,
26 Northwestern University, 1800 Sherman Ave, Evanston, IL 60201, USA

27 ⁴LIGO, Massachusetts Institute of Technology, Cambridge, MA 02139, USA

28 ⁵Kavli Institute for Cosmological Physics, The University of Chicago, 5640 South
29 Ellis Avenue, Chicago, IL 60637, USA

30 ⁶Enrico Fermi Institute, The University of Chicago, 933 East 56th Street, Chicago,
31 IL 60637, USA

32 ⁷SUPA, School of Physics and Astronomy, University of Glasgow, Kelvin Building,
33 University Ave, Glasgow G12 8QQ, UK

35 ⁸Nicholas and Lee Begovich Center for Gravitational-Wave Physics and Astronomy
36 (GWPAC), Department of Physics, California State University Fullerton, Fullerton,
37 800 North State College Blvd, CA 92831, USA

38 ⁹Microsoft Corporation, Mountain View, CA, USA

39 ¹⁰Microsoft Corporation, Redmond, WA, USA

40 ¹¹School of Information Studies, Syracuse University, 343 Hinds Hall, Syracuse, NY
41 13210, USA

42 ¹²Zooniverse, The Adler Planetarium, 1300 South DuSable Lake Shore Drive,
43 Chicago, IL, 60605, USA

44 ¹³Electrical and Computer Engineering, Northwestern University, 2145 Sheridan
45 Road, Evanston, IL 60208, USA

46 E-mail: christopher.berry.2@glasgow.ac.uk

51 **Abstract.** Understanding the noise in gravitational-wave detectors is central to
52 detecting and interpreting gravitational-wave signals. Glitches are transient, non-
53 Gaussian noise features that can have a range of environmental and instrumental
54 origins. The Gravity Spy project uses a machine-learning algorithm to classify glitches
55 based upon their time–frequency morphology. The resulting set of classified glitches
56 can be used as input to detector-characterisation investigations of how to mitigate
57 glitches, or data-analysis studies of how to ameliorate the impact of glitches. Here
58 we present the results of the Gravity Spy analysis of data up to the end of the third
59 run.

60 Accepted

1
2 *Gravity Spy O3 data set* 2
3
4
5
6
7
8
9
10
11
12
13

observing run of Advanced LIGO. We classify 233981 glitches from LIGO Hanford and 379805 glitches from LIGO Livingston into morphological classes. We find that the distribution of glitches differs between the two LIGO sites. This highlights the potential need for studies of data quality to be individually tailored to each gravitational-wave observatory.

14 Submitted to: *Class. Quantum Grav.*15
16 **1. Introduction**
17
18

19 Gravitational-wave astronomy provides unique information about our Universe. To
20 date, the Advanced Laser Interferometric Gravitational-Wave Observatory (LIGO) [1]
21 and Advanced Virgo [2] detectors have observed signals from coalescing binaries of
22 neutron stars and black holes [3-7], with the rate of discovery increasing dramatically
23 as the sensitivity of the detector network improves. Analysis by the LIGO Scientific,
24 Virgo and KAGRA (LVK) Collaboration identified 3 candidates with a probability of
25 astrophysical origin greater than 50% in the first observing run (O1) of the advanced-
26 detector network [8], 8 in the second observing run (O2) [4], and 79 in the third observing
27 run (O3) [6,7]. Such observations require measurements equivalent to fractional changes
28 in distance of $\lesssim 10^{-21}$ [9], and hence the detector must be carefully isolated from
29 instrumental and environmental sources of noise. However, noise cannot be fully
30 eliminated, and to identify and analyse gravitational-wave signals it is necessary to
31 understand the properties of noise in the gravitational-wave detectors [10].
32
33

34 Transient, non-Gaussian bursts of noise (typically less than a few seconds in
35 duration) in the gravitational-wave data stream are known as *glitches*. Glitches
36 are particularly detrimental to the identification and analysis of gravitational-wave
37 signals [10-16]. There are many different glitch types, some with known environmental
38 or instrumental origins, and others with uncertain or unknown sources [17-21].
39 Identifying the causes of glitches is key to improving gravitational-wave data quality.

40 A wide range of tools are used to monitor data quality and characterise the
41 behaviour of the detectors [20-27]. In recent years, machine-learning methods have
42 been developed for a range of analyses connected to various aspects of detector
43 characterisation [e.g., 28-38]. The Gravity Spy project [39-42] aims to classify glitches
44 by combining human and machine-learning classification schemes: volunteers on the
45 Zooniverse citizen-science platform (as well as LVK detector-characterisation experts)
46 inspect and classify individual glitches, which can then be used as input to a machine-
47 learning algorithm that can classify large sets of data.‡ Since its launch in October
48 2016, the Gravity Spy project has analysed almost 2 million individual glitches and has
49 accumulated over 5.7 million classifications by more than 27,000 registered Zooniverse
50
51
52
53
54
55
56
57
58
59
60

‡ Gravity Spy Zooniverse project gravityspy.org.

1
2 *Gravity Spy O3 data set*
3
45 users. § Results of machine-learning and volunteer classifications have been made
6 available both internally within the LVK, and to the wider public [44–47].
78 Compiling a catalogue of classified glitches is useful for both identifying the
9 physical causes of glitches (such that commissioning work could be done to remove
10 them), and evaluating the impact of glitches on data analysis (creating new analyses
11 to mitigate their effect where necessary). For example, Gravity Spy classifications
12 have been used for: selecting example glitches to evaluate their impact on data
13 analysis [48–51]; studying glitch morphology [52–55]; cross-referencing glitches with
14 environmental-noise or auxiliary-channel measurements [20, 56–58], and as a component
15 of training for gravitational-wave detection algorithms [59–65] or glitch-classification
16 algorithms [32, 66–69]. Additionally, identification of new classes can indicate new
17 sources of noise and suggest areas for further commissioning [42].
1819 In this paper we describe the glitch classifications from Gravity Spy’s machine-
20 learning analysis of data from the first three observing runs of Advanced LIGO; this
21 analysis uses the Gravity Spy convolutional neural network (CNN) models previously
22 developed for O1–O2 [39, 40] and O3 [42]. In Section 2 we describe the gravitational-
23 wave strain data, the machine-learning algorithm and the glitch classes; further details
24 of the different classes used for analysis of each observing run are given in Appendix A.
25 In Section 3 we illustrate how results of classifications from across the observing runs
26 can be used for detector characterisation, summarising the rates of different glitches,
27 and highlighting results from times near potential gravitational-wave candidates; we
28 also give an overview of the data release. In Section 4 we review the implications of our
29 results, before summarising in Section 5. The data release is available from Zenodo [46],
30 and the volunteer classifications [47] will be discussed in a companion paper.
3132
33

2. Methods

3435

2.1. *Detector data & detector characterisation*

3637 The two LIGO detectors in the USA (Hanford and Livingston) [1], the Virgo detector
38 in Italy [2] and the KAGRA detector in Japan [70], are highly sensitive instruments
39 designed and operated for the direct detection of gravitational waves. The primary data
40 output of these observatories is the strain measured by the interferometers [71], which
41 will contain gravitational-wave signals as well as various sources of noise; however, there
42 are additionally many auxiliary channels of data that record the internal state of the
43 detectors and monitor their environments [17, 72, 73]. Since the beginning of O1 in
44 September 2015, three observing runs have been completed [74]. These are preceded
45 and interleaved with engineering runs that are used to test the performance of the
46 detectors, and potentially diagnose data-quality issues. Each successive observing run
47 is characterised by detector improvements that lead to higher sensitivity [75–78] and,
4849
50
51
52
53
54
55
56
57
58
59
60
§ The European Gravitational Observatory run a similar project dedicated to understanding glitches
in Virgo data: GWitchHunters [43] www.zooniverse.org/projects/reinforce/gwitchhunters.

1
2 *Gravity Spy O3 data set*
3
45 consequently, more detections [7], as well as revealing new sources of noise.
67 The data quality of these ground-based gravitational-wave detectors is impacted by
8 multiple sources of noise. Broadly, noise in the detectors consists of stationary Gaussian
9 noise sources (which include quantum noise, seismic noise and thermal noise), and non-
10 Gaussian noise sources [10, 72, 76, 78]. Non-Gaussian noise includes long-lived spectral
11 lines [79] and shorter-duration transient glitches [20, 22, 23]. Monitoring the status
12 of data quality, identification and mitigation of transient noise are some of the tasks
13 referred to as detector characterisation [17, 21]. Understanding and improving data
14 quality is central to extracting astrophysical information from detector data.
1516 Potential glitches (as well as gravitational-wave signals) are identified by searching
17 for excess power in the data stream. All the noise transients analyzed in this paper
18 were detected by the Omicron algorithm [26, 27] analysing the gravitational-wave strain
19 channel (and not using auxiliary channels). Omicron identifies potential noise transients
20 by triggering on excess power in the data stream. The Omicron algorithm annotates
21 each identified transient with characteristics such as event time, peak frequency, central
22 frequency and signal-to-noise ratio (SNR). The glitch morphology of the trigger can be
23 visualized in a time–frequency spectrogram commonly known as an Omega scan [25, 80].
24 These Omega scans are used frequently in data-quality studies to establish potential
25 noise correlations between different parts of the detector [81], and the time–frequency
26 morphology can be used to categorise glitches [20, 40]. The morphology may contain
27 clues to the cause of the glitch [21], e.g., arches are characteristic of light scattering,
28 with the frequency encoding information about the relative motion of the scattering
29 source, and multiple stacked arches suggesting repeated reflections of stray light from
30 the scattering source [56, 82, 83]. Example Omega scans for common glitch classes are
31 shown in Figure 1. These time–frequency spectrograms are used as the input to Gravity
32 Spy.
3334 *2.2. Machine-learning algorithm & glitch classes*
35
3637 Gravity Spy contributes to detector characterisation by classifying glitches. The
38 morphological classes used in Gravity Spy for LIGO data are detailed in Appendix
39 A. Classifications are made based upon time–frequency spectrograms, using two
40 complementary approaches: visual inspection by Zooniverse volunteers, and automated
41 analysis by a machine-learning algorithm [39, 41, 42]. Both approaches use the same
42 input: Omega scans of four different temporal resolutions (0.5 s, 1 s, 2 s and 4 s in
43 duration, centred on the time of the transient). Here we concentrate on the machine-
44 learning classification as opposed to volunteer classification.
4546 Gravity Spy uses a CNN, a deep-learning algorithm used primarily for image
47 classification, to analyse the Omega scans. For every image input to the CNN, the
48 probability (or *confidence*) p of belonging to each class is calculated, and the glitch is
49 assigned to the class with the highest associated confidence [39]. CNN architectures
50 include an input layer, an output layer, and various hidden layers in between that
5152
53
54
55
56
57
58
59
60

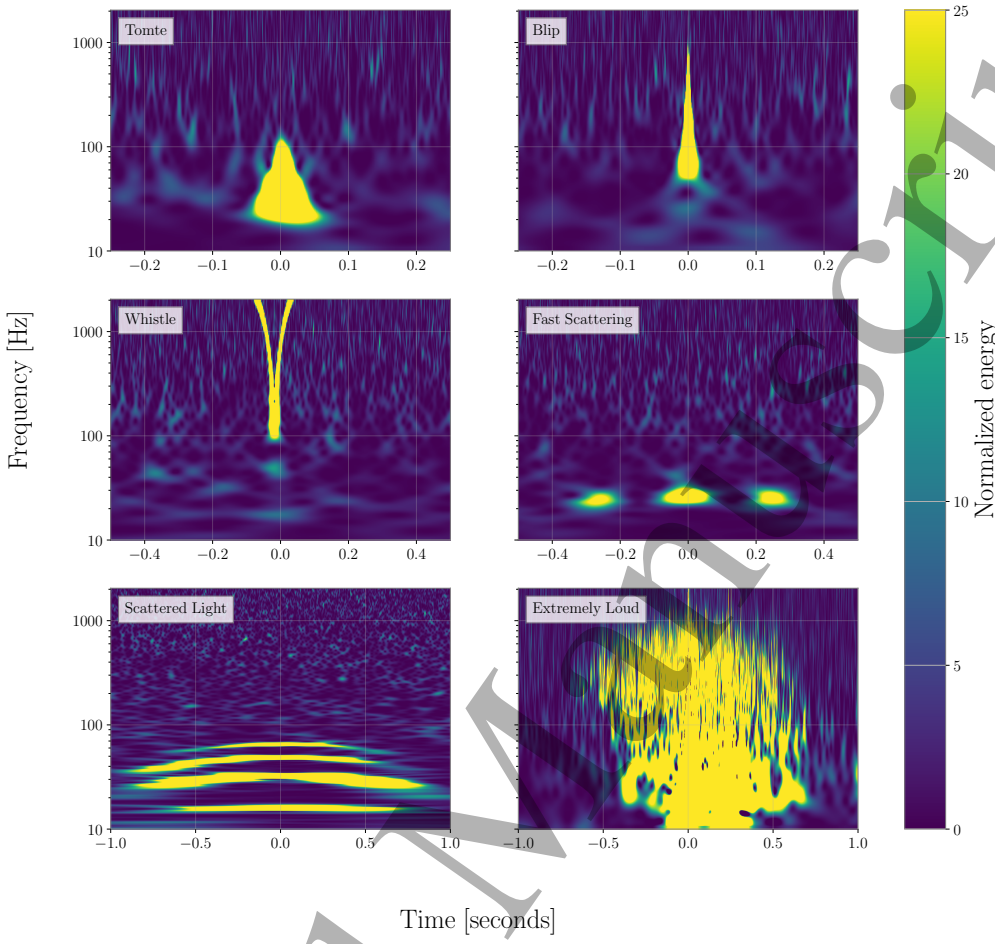
1
2 *Gravity Spy O3 data set*
3
4

Figure 1: Example time–frequency spectrograms [80] for a selection of LIGO glitch classes. The glitch classes here are relatively common and illustrate the range of morphologies different glitch classes can have. The spectrograms in each row are shown with a different time duration. *Top left*: Tomte is a short-duration glitch with a characteristic triangular morphology. *Top right*: Blip is another short-duration glitch, but covers a broader frequency range than Tomte and has a tear-drop morphology. *Middle left*: Whistles have a characteristic V, U or W shape sweeping through higher frequencies ($\gtrsim 128$ Hz). *Middle right*: Fast Scattering (also known as Crown) appears as one or more arches, each ~ 0.2 – 0.3 s in duration. *Bottom left*: Scattered Light (also known as Slow Scattering) appears as longer-duration (~ 2.0 – 2.5 s) arches, with multiple arches often being stacked on top of each other. *Bottom right*: Extremely Loud are high-SNR triggers that saturate the spectrogram. Exemplar spectrograms for each Gravity Spy class are given in Figure A1.

1
2 *Gravity Spy O3 data set*
3
45 transform the data and extract useful features. The CNN used by Gravity Spy [84]
6 has four convolutional layers to extract features, each followed by a max-pooling and a
7 rectified linear unit (ReLU) activation layer, and then a final fully connected layer and
8 a softmax layer. The weights from the last softmax layer are the confidence scores for
9 each of the classes. Confidence scores for each trigger, indicating the probability that it
10 is associated with various morphological classes, are provided in the data release. The
11 accuracy of the classification is tested during training of the CNN [39, 42, 84].
12
1314
15 *2.3. The training sets*
1617 The original LIGO data set used to train the Gravity Spy CNN was created by
18 detector-characterisation experts and Gravity Spy volunteers. It initially contained 7718
19 glitch samples from 20 classes prevalent in the detector during O1 and the preceding
20 engineering runs [39]. These classes included No Glitch, for when no significant excess
21 power is visible in the Gravity Spy spectrograms, and None of the Above, which was
22 intended to catch glitches that did not fit into the other classes. The training set was
23 refined and updated to include the 1080 Lines and 1400 Ripples classes, which were
24 identified by volunteers [40]. This gave a training set that included 7932 glitch samples
25 from 22 classes [45]. The resulting training accuracy was 98.2% [40]. This CNN model
26 has been used to classify data from O1 and O2.
27
2829 During O3, the presence of two new prevalent glitch morphologies motivated the
30 addition of the Fast Scattering (also known as Crown) and Blip Low Frequency (also
31 known as Low-frequency Blip) classes to the machine-learning model; in addition, the
32 None of the Above class was removed for the final analysis, as it was decided that it
33 was more effective for the CNN to label such triggers with low confidence than to try
34 to construct a class of many morphologically diverse glitches [42].^{||} Adding in the new
35 classes, and more examples from existing classes, this current training data set contains
36 9631 glitch samples distributed over 23 classes, of these 8427 were used for training and
37 1203 were used for validation. The resulting training and validation accuracies were
38 99.9% and 98.8%, respectively [42]. This CNN model has been used to classify data
39 from O3.
40
4142 The performance of the CNN model depends upon the quantity and quality of
43 examples from each glitch class in the training set. Augmenting the training set with
44 additional glitches classified by volunteers [47] is expected to improve the results of
45 future CNN models.
4647
48
49
50
51 ^{||} None of the Above remains an option for Zooniverse volunteers. We anticipate that reinstating the
52 None of the Above class may be useful for identifying new classes in preliminary analysis of future
53 observing runs. Prior to the introduction of the Fast Scattering class, there were a large number of
54 None of the Above classifications for O3 data with the characteristic Fast Scattering morphology [42].
55
56
57
58
59
60

1
2 *Gravity Spy O3 data set*
3
4
56 **3. Results**
7
8
9
10
11
12
13
14

The Gravity Spy glitch classifications can be used as inputs for a range of analyses, and here we illustrate their use as the base for detector-characterisation studies concentrating on O3. In Sec. 3.1 we show how the distribution of glitches may be studied, and in Sec. 3.2 we illustrate how data quality at specific times may be studied using the example of times around gravitational-wave candidates. For use in further studies, the release of the Gravity Spy machine-learning classification data set is described in Sec. 3.3.

15
16 *3.1. Glitch classifications*
17
18
19
20
21
22
23
24
25
26
27
28

For data from both LIGO detectors, we find that there are certain glitch classes that are more common than others. For example, Table 1 provides numbers of glitches sorted into the various classes from O3 data. In addition to the number of glitches in each class with an SNR > 7.5 , we also show those classified with a confidence $> 90\%$ and $> 95\%$. Using a higher confidence level gives a higher purity, but smaller sample. Figure 2 shows the cumulative distribution of classifications as a function of confidence; this gives an indication of how the numbers change with a different confidence thresholds. We mainly use a fiducial 90% confidence threshold for our quoted results.

The number of glitches and the split between classes differs between the two observatories. Figure 3 shows the O3 distribution of glitches as a function of SNR for the most common classes (classes that have a $> 1\%$ prevalence) in LIGO Hanford data, and Fig. 4 shows the same for LIGO Livingston.

During O3, the most common classes of glitches to occur at Livingston was due to scattered light [82, 83, 85], specifically, Scattered Light (also known as Slow Scattering) [56] and Fast Scattering (also known as Crown) [42]. Approximately 27% of all the glitches in O3 were classified as Fast Scattering by the Gravity Spy machine-learning analysis with a confidence of $> 90\%$. Scattered Light made up about 23% of glitches with a Gravity Spy confidence of $> 90\%$. The relative motion between optical surfaces in LIGO are strongly correlated with the presence of light scattering. The rate of Scattered Light glitches decreased during the second half of O3 (O3b) following the introduction of reaction-chain tracking in January 2020 [7], which reduced the relative motion between the test-mass mirror and its counterpart used in control of the suspension system [56].

Tomtes were another common glitch class for Livingston, making up approximately 19% of all the glitches with a Gravity Spy confidence of $> 90\%$. The origins of these are currently unknown, as no environmental or instrumental couplings have been determined. They commonly appear with a frequency of 40 Hz, and repeat often over the course of one day [20].

At Hanford, Scattered Light, Low-frequency Bursts, and Extremely Loud glitches were the most common glitch classes. Reaction-chain tracking was also implemented at Hanford to help mitigate Scattered Light. Low-frequency Bursts were common during August 2019. Extremely Loud glitches are large disturbances to the detector and often

1
2 *Gravity Spy O3 data set*
3
4

Gravity Spy class	Hanford			Livingston		
	SNR > 7.5	$p > 90\%$	$p > 95\%$	SNR > 7.5	$p > 90\%$	$p > 95\%$
1080 Lines	344	78	34	942	269	141
1400 Ripples	253	85	49	7634	2384	1479
Air Compressor	343	117	76	2901	1314	952
Blip	7438	6020	5582	5554	4264	3873
Blip Low Frequency	4042	2467	2059	21522	15614	14003
Chirp	41	8	5	29	12	8
Extremely Loud	13235	10938	10335	8994	7304	6835
Fast Scattering	2243	1286	1118	74120	55211	50782
Helix	91	15	9	229	37	16
Koi Fish	11242	8447	7536	11153	7016	5800
Light Modulation	146	45	29	753	191	133
Low-frequency Burst	21211	19410	18756	5771	3855	3448
Low-frequency Lines	3955	1536	1131	13749	3751	2125
No Glitch	7783	5247	3874	14050	6748	4773
Paired Doves	269	29	12	4079	277	130
Power Line	303	164	135	1985	1441	1314
Repeating Blips	1845	1078	902	1142	459	350
Scattered Light	63333	57118	53701	57400	47258	43009
Scratchy	643	367	311	444	287	263
Tomte	1892	1360	1242	46144	39299	37573
Wandering Line	30	10	5	64	28	20
Whistle	6238	5371	5128	8623	6150	5721
Violin Mode	884	436	366	1709	300	190

32
33 Table 1: Number of Gravity Spy classifications in O3 LIGO Hanford and Livingston
34 data. For each detector, the left column gives the total number of triggers with SNR
35 > 7.5 classified, regardless of the confidence of the classification, while the middle and
36 right columns give the number of classifications with confidence $p > 90\%$ (our fiducial
37 threshold) and $p > 95\%$, respectively.
38
39

40
41 cause big drops in the detector’s astrophysical range (the distance out to which a source
42 can be typically detected [86]). Scattered Light made up about 47% of O3 glitches
43 classified with $> 90\%$ confidence at Hanford, while Extremely Loud and Low-frequency
44 Bursts made up about 9% and 16%, respectively.
45
46

47 Figure 5 shows the hourly rate of four glitch classes (Scattered Light, Fast
48 Scattering, Low-frequency Burst and Tomte) across the weeks of the O3 run for both
49 Hanford and Livingston [5, 7]. The rate is calculated per unit observing time. The
50 glitch rates were calculated using those classified with $> 90\%$ confidence. This shows
51 the large increase in Scattered Light glitches in the second part of the observing run and
52 the subsequent reduction after the introduction of reaction-chain tracking [7, 20, 56].
53
54

55 Figure 6 shows a different visualization of the variation in glitch prevalence with
56 time: how the glitch rate (for the same classes shown in Fig. 5) changes with the day of
57 the week. Fast Scattering shows a decline during the weekend at LIGO Livingston, as
58

59 Plotting the number of glitches (the glitch rate multiplied by the detector duty cycle) instead of
60

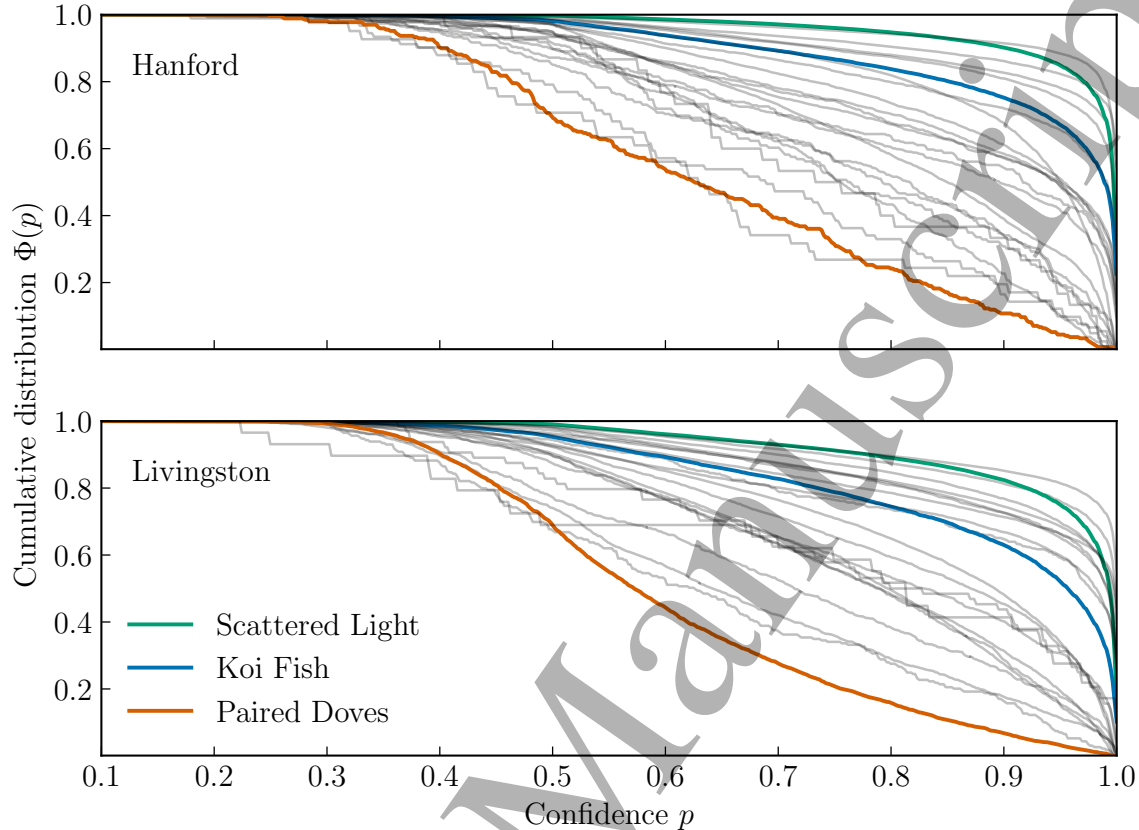
1
2
3
4
5
6
7
8
9
10
11
12
13
14
15
16
17
18
19
20
21
22
23
24
25
26
27
28
29
30
31
32
33
34
35
36
37
38
39
40
41
42
43
44
45
46
47
48
49
50
51
52
53
54
55
56
57
58
59
60

Figure 2: The cumulative distribution of O3 triggers across all classes as a function of classification confidence. The horizontal axis is the confidence p , while the vertical axis $\Phi(p)$ is the fraction of glitches identified with confidence *greater* than p . Three glitch classes are highlighted as examples: Paired Doves (an uncommon class, with few training examples [39, 40]), Koi Fish (a more common class, which can be confused with Blips when quiet, and Extremely Loud when loud [40, 42]), and Scattered Light (one of the most common glitch types for both detectors [42]). The number of triggers in each class with $p > 0.9$ and $p > 0.95$ are quoted in Table 1.

at these times there is less anthropogenic noise around the detectors. A similar difference is not visible at LIGO Hanford because of the much lower rate of Fast Scattering transients at Hanford (0.22 per hour) compared to Livingston (9.05 per hour) during O3: a relatively higher ground motion in the anthropogenic band around Livingston makes Fast Scattering a much bigger problem there [7, 42]. In contrast to Fast Scattering, Tomte shows negligible variation, indicating a lack of correlation with human activities.

the glitch rate, would show a significant drop on Tuesdays, as this corresponds to the day of routine maintenance.

Gravity Spy O3 data set

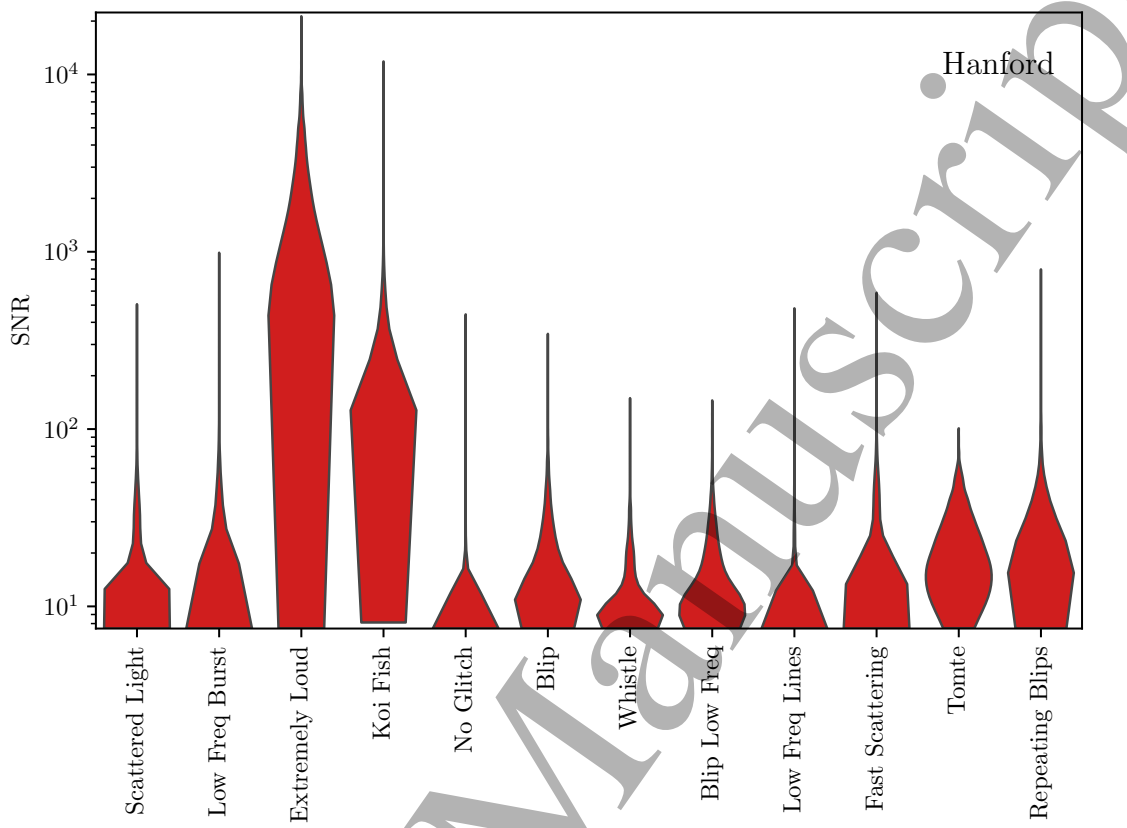


Figure 3: SNR distributions for LIGO Hanford glitches identified with a confidence $p > 90\%$. Only results for classes with a prevalence greater than 1% in Hanford data are shown. The width of the distribution is normalized to be uniform across the different classes, and the classes are ordered in decreasing order of prevalence from left to right. Table 1 lists the numbers of triggers in each class for the full list of classes, and analogous distributions for Livingston data are shown in Fig. 4.

3.2. Data quality around candidates

The data set includes glitch classifications for data around the time of several gravitational-wave candidates. This happens either when there is a glitch picked up by Omicron, if a gravitational-wave signal is loud enough to trigger Omicron, or if some combination of glitch and signal is identified. Here we review these Gravity Spy classifications, and illustrate both how Gravity Spy may identify glitches around candidates and how it may struggle in classifying a gravitational-wave signal.

Table 2 and Table 3 provide details of example candidates from the first and second parts of O3 (O3a and O3b), respectively, with associated Gravity Spy classifications. This list was compiled by cross-referencing the times associated with public alerts and high-significance candidates from offline analyses (whether or not they are identified as instrumental in origin) [5, 7, 87, 92] with the Gravity Spy data set. For this analysis, a time window of ± 5 s around each candidate time was used to search for entries in the

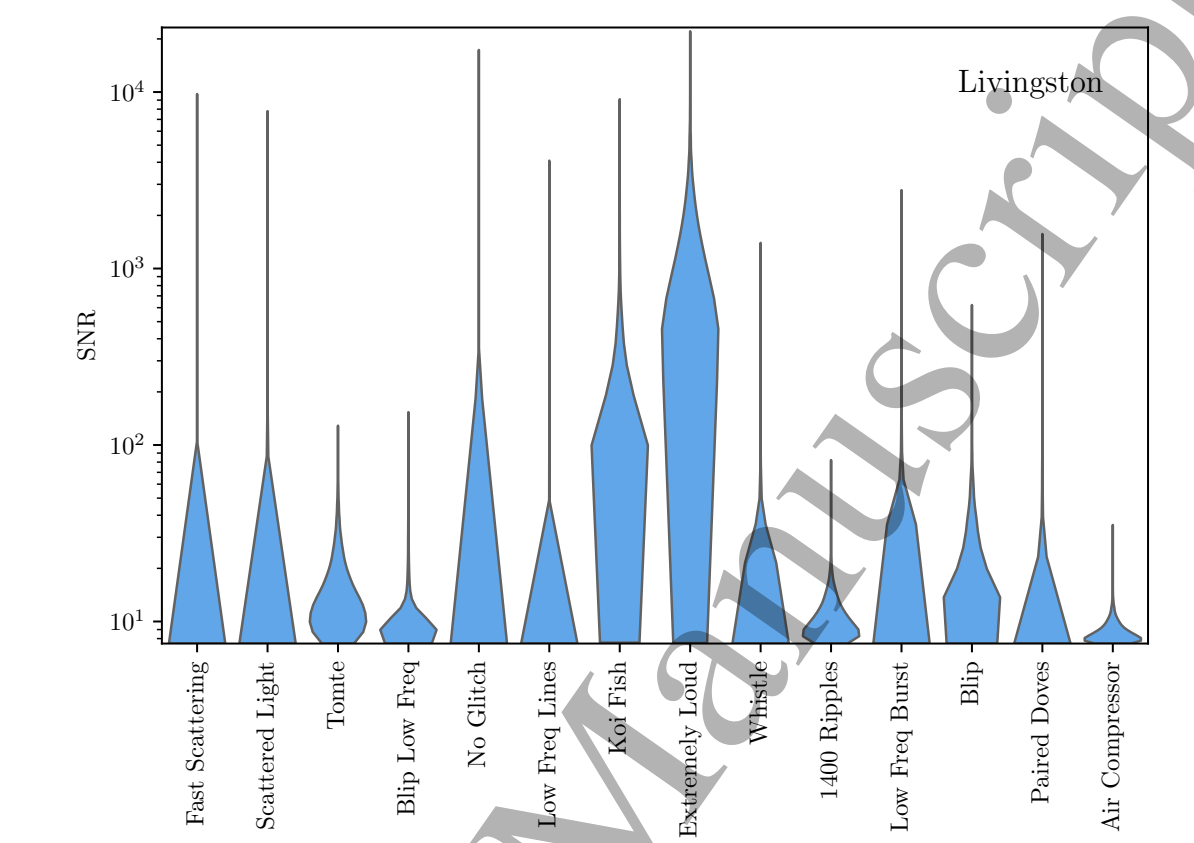
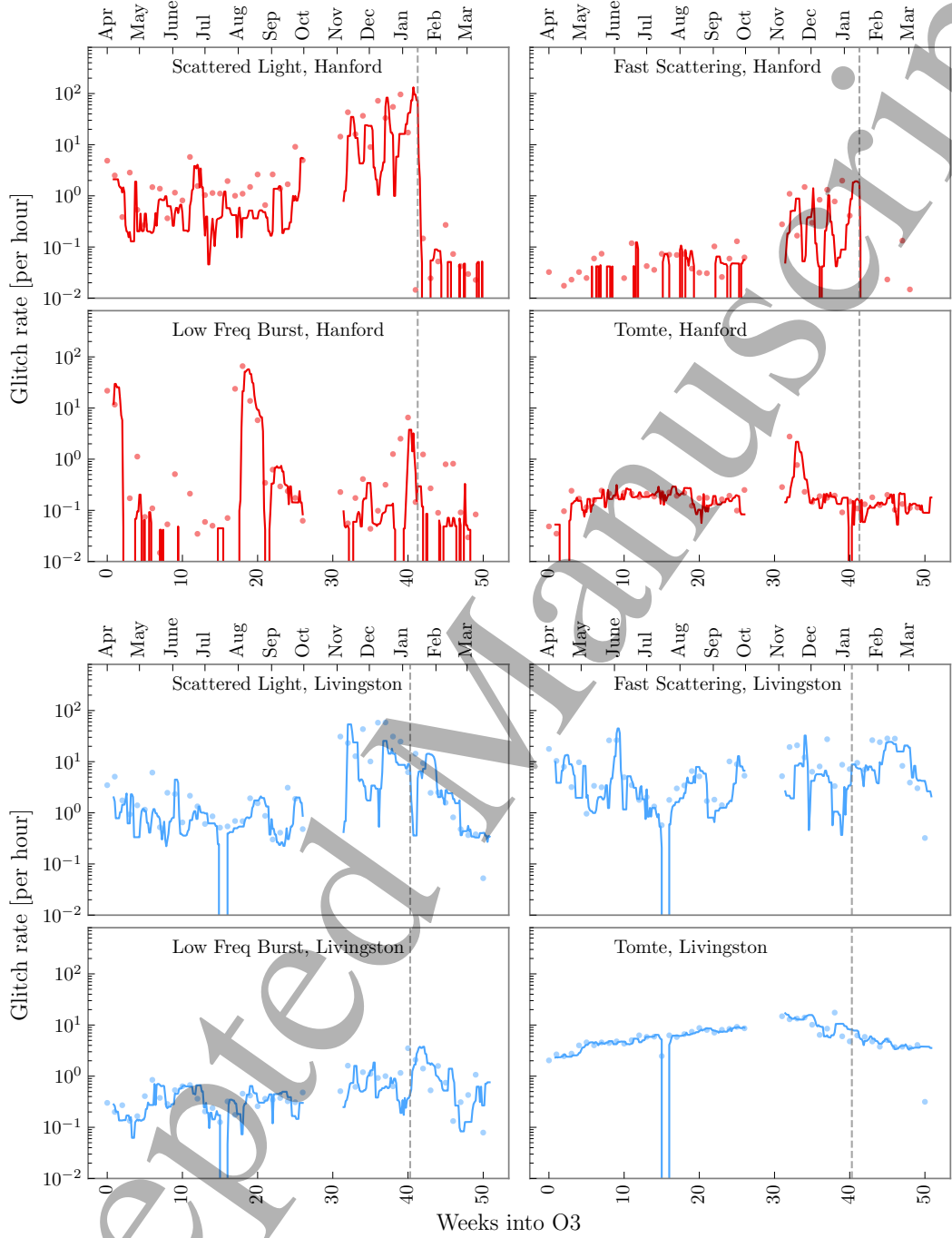
1
2
3
4
5
6
7
8
9
10
11
12
13
14
15
16
17
18
19
20
21
22
23
24
25
26
27
28
29
30
31
32
33
34
35
36
37
38
39
40
41
42
43
44
45
46
47
48
49
50
51
52
53
54
55
56
57
58
59
60

Figure 4: SNR distributions for LIGO Livingston glitches identified with a confidence $p > 90\%$. Only results for classes with a prevalence greater than 1% in Livingston data are shown. The width of the distribution is normalized to be uniform across the different classes, and the classes are ordered in decreasing order of prevalence from left to right. Table 1 lists the numbers of triggers in each class for the full list of classes, and analogous distributions for Hanford data are shown in Fig. 4.

Gravity Spy data set. The majority of candidates did not have a corresponding entry in the data set classified by Gravity Spy.

First, we consider the set of classifications around gravitational-wave candidates without an identified instrumental origin:

- From Livingston, there are 14 O3a candidates that have at least one trigger identified by Gravity Spy, and 7 O3b candidates. Three of the O3b events had two Livingston triggers during the time of the candidate. The most common class of glitches found were Chirps. Fast Scattering, Blip and Tomte were other common classifications.
- At Hanford, only 7 candidates from O3 are part of the Gravity Spy data set. One of these candidates has three associated Hanford glitches, and another has two. The most common class to occur at times associated with these candidates was Scattered Light.

1
2 *Gravity Spy O3 data set*
3
4

49
50 Figure 5: Hourly glitch rate (per unit observing time) for four glitch types (classified with
51 confidence $> 90\%$) at LIGO Hanford and LIGO Livingston during O3 on different days
52 of the week. The rate is calculated as the number of glitches per unit observing time.
53 The solid traces show the rolling median of the daily average glitch rate across seven
54 day intervals, while the dots show the glitch rate for each calendar week. The dashed
55 vertical lines show the times when reaction-chain tracking was implemented [7, 56]. The
56 month of October was used for commissioning, and its data is not shown here.
57
58
59
60

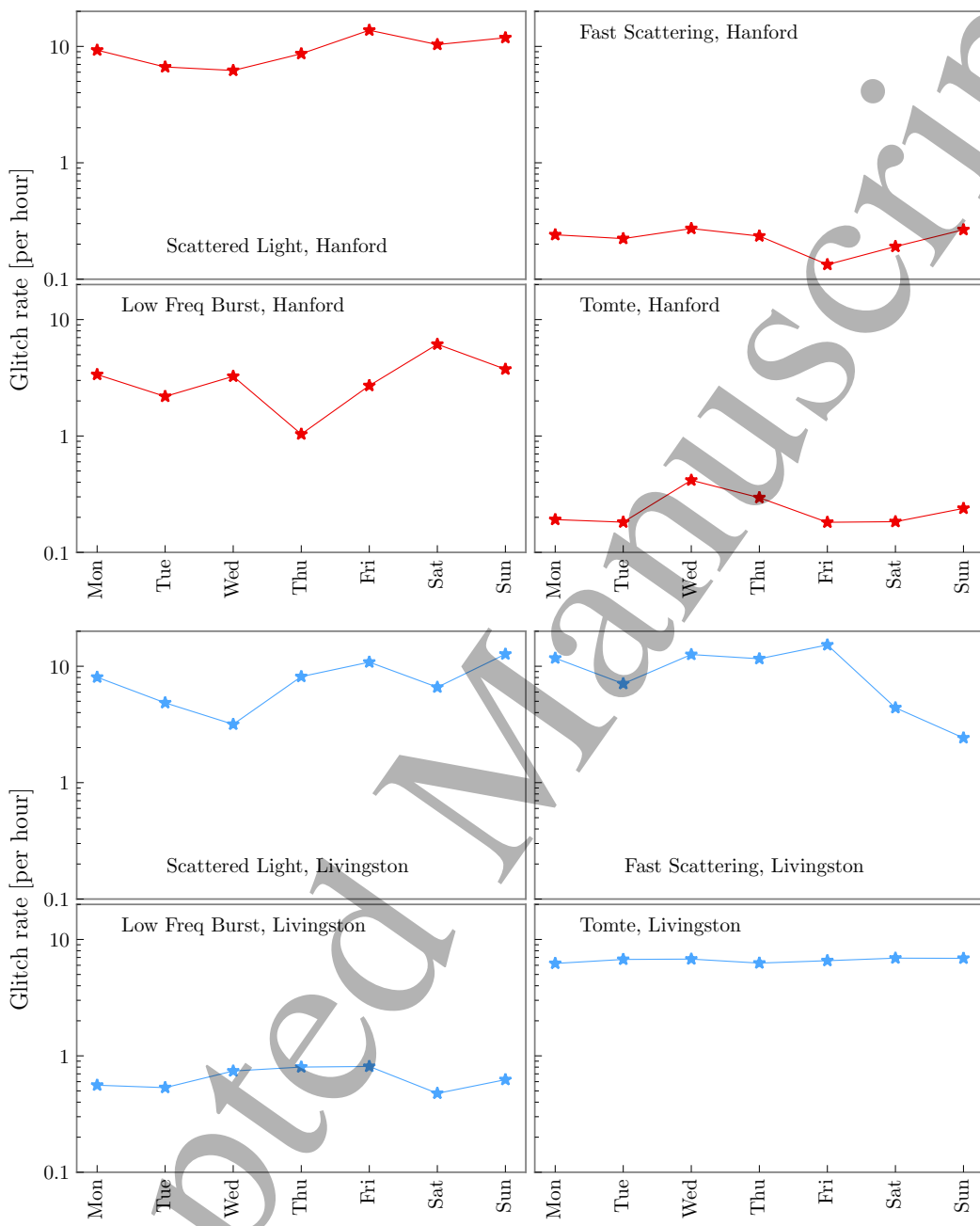
1
2 *Gravity Spy O3 data set*
3

Figure 6: Hourly glitch rate for weekdays folded across the entire O3 run. The rate is calculated as the number of glitches per unit observing time, and we plot the average over each weekday. The month of October was used for commissioning and its data is not shown here.

1
2 *Gravity Spy O3 data set*
3
4

14

Superevent	Time	Gravity Spy classification	Description
S190930ak	2019-09-30 23:46:50	H: Scattered Light	Instrumental origin [7]
	2019-09-30 23:46:53	H: Scattered Light	
S190930s	2019-09-30 13:35:37	L: Low Frequency Lines	GW190930_133541 [5, 93]
S190928c	2019-09-28 02:11:45	L: Tomte	Retracted [5, 94]
S190924am	2019-09-24 23:26:50	L: Fast Scattering	Instrumental origin [87]
	2019-09-24 23:26:52	L: Fast Scattering	
	2019-09-24 23:26:54	L: Fast Scattering	
S190924h	2019-09-24 02:18:42	L: Tomte	GW190924_021846 [5, 95]
S190910s	2019-09-10 11:28:07	L: Chirp	GW190910_112807 [5]
S190904w	2019-09-04 17:49:10	L: Fast Scattering	Instrumental origin [90]
S190829u	2019-08-29 21:05:56	L: Koi Fish	Retracted [5, 96]
S190814bv	2019-08-14 21:10:38	L: Scattered Light	GW190814_211038 [5, 97, 98]
S190808ae	2019-08-08 22:21:21	H: Low Frequency Burst	Retracted [5, 99]
S190804q	2019-08-04 08:35:43	L: Koi Fish	Instrumental origin [7, 88]
S190803e	2019-08-03 02:26:59	H: Low Frequency Burst	GW190803_022701 [5]
S190728q	2019-07-28 06:45:12	L: No Glitch	GW190728_064510 [5, 100]
S190701ah	2019-07-01 20:33:02	L: Fast Scattering	GW190701_203306 [5, 101]
S190630ag	2019-06-30 18:52:05	L: Chirp	GW190630_18520 [5, 102]
S190524q	2019-05-24 04:52:01	L: No Glitch	Retracted [5, 103]
	2019-05-24 04:52:02	L: No Glitch	
	2019-05-24 04:52:04	L: No Glitch	
	2019-05-24 04:52:09	L: No Glitch	
S190521r	2019-05-21 07:43:59	H: Blip, L: Chirp	GW190521_074359 [5, 104]
S190521g	2019-05-21 03:02:29	L: Blip Low Frequency	GW190521 [5, 105, 106]
S190519bj	2019-05-19 15:35:44	L: Blip	GW190519_153544 [5, 107]
S190512at	2019-05-12 18:07:18	L: Tomte	GW190512_180714 [5, 108]
S190430af	2019-04-30 00:49:32	H: Koi Fish	Instrumental origin [88]
S190421ar	2019-04-21 21:38:53	L: Power Line	GW190421_213856 [5, 109]
S190413ac	2019-04-13 13:43:10	L: Fast Scattering	GW190413_134308 [5]
S190412m	2019-04-12 05:30:44	L: Chirp	GW190412 [5, 110, 111]
S190408an	2019-04-08 18:18:06	H: Low Frequency Burst	GW190408_181802 [5, 112]

40 Table 2: Gravity Spy classifications coincident with confident, marginal and retracted
41 O3a gravitational-wave candidates [5, 7, 87, 92]. Equivalent results for O3b are shown
42 in Table 3. The main Gravity Spy analysis uses data flagged by the Omicron pipeline
43 as an input, and so only classifies a subset of candidates. Omicron may pick up the
44 candidate, a near-by glitch, or some combination of the two. The first column gives the
45 corresponding candidate identification used in the Gravitational-wave Candidate Event
46 Database (as used for low-latency alerts); the second gives the Coordinated Universal
47 Time of the Omicron trigger (± 5 s from the time of the candidate); the third column
48 gives the Gravity Spy classification with H and L indicating whether data from Hanford
49 or Livingston, respectively, have been analysed; the fourth column gives details of the
50 final status of the candidate (and citations).
51
52
53
54

1
2 *Gravity Spy O3 data set* 15
3

5	Superevent	Time	Gravity Spy classification	Description
6	S200311bg	2020-03-11 11:58:53	L: Blip	GW200311_115853 [7, 113]
7	S200224ca	2020-02-24 22:22:34	H: Blip, L: Chirp	GW200224_222234 [7, 114]
8	S200214br	2020-02-14 22:45:26	L: Fast Scattering	Instrumental origin [7, 87]
9	S200129m	2020-01-29 06:55:00	L: Fast Scattering	GW200129_065458 [7, 115]
10		2020-01-29 06:54:58	H + L: Chirp	
11	S200121aa	2020-01-21 03:17:48	H: Blip	Instrumental origin [7]
12	S200116ah	2020-01-16 11:56:12	L: Tomte	Retracted [116]
13	S200114f	2020-01-14 02:08:18	L: Tomte	Instrumental origin [87, 88, 117]
14	S200112r	2020-01-12 15:58:38	L: Chirp	GW200112_155838 [7, 118]
15	S200108v	2020-01-08 10:00:38	L: Extremely Loud	Retracted [119]
16	S200106av	2020-01-06 18:34:32	H + L: Scattered Light	Retracted [7, 120]
17	S191225aq	2019-12-25 21:57:15	L: Tomte	Retracted [87, 121]
18	S191223an	2019-12-23 01:41:59	L: Tomte	Instrumental origin [87]
19	S191213g	2019-12-13 04:34:08	L: Scattered Light	Unretracted, low significance [7, 122]
20	S191212q	2019-12-12 08:27:25	H: Scattered Light	Retracted [123]
21		2019-12-12 08:27:28	H: Scattered Light	
22	S191127p	2019-11-27 05:02:28	H: Scattered Light	GW191127_050227 [7]
23		2019-11-27 05:02:24	H: Scattered Light	
24	S191120aj	2019-11-20 16:23:24	L: Air Compressor	Retracted [124]
25	S191117j	2019-11-17 06:08:22	L: Extremely Loud	Retracted [125]
26	S191113q	2019-11-13 07:17:53	L: No Glitch	GW191113_071753 [7]
27		2019-11-13 07:17:48	L: No Glitch	
28	S191110x	2019-11-10 18:08:42	L: Koi Fish	Retracted [126]
29	S191109d	2019-11-09 01:07:17	H: Scattered Light, L: Blip	GW191109_010717 [7, 127]
30		2019-11-09 01:07:15	H: Scattered Light	
31		2019-11-09 01:07:13	L: Scattered Light	
32		2019-11-09 01:07:12	H: Scattered Light	
33	S191103a	2019-11-03 01:25:52	L: Tomte	GW191103_012549 [7]
34				
35				

37 Table 3: Gravity Spy classifications coincident with confident, marginal and retracted
38 O3b gravitational-wave candidates [7, 87, 90, 92]. This is equivalent to Table 2 but
39 for O3b. The first column gives the corresponding candidate identification used in
40 the Gravitational-wave Candidate Event Database; the second gives the Coordinated
41 Universal Time of the Omicron trigger (± 5 s from the time of the candidate); the third
42 column gives the Gravity Spy classification with H and L indicating whether data from
43 Hanford or Livingston, respectively, have been analysed; the fourth column gives details
44 of the final status of the candidate (and citations).
45

46

- 47 • There were 4 candidates in which a glitch was found at both detectors:
48 GW190521_074359, GW191109_010717, GW200129_065458 and GW200224_222234.
49 GW190521_074359, GW200129_065458 and GW200224_222234 are amongst
50 the highest SNR candidates from O3 [5, 7]. GW190521_074359 [5] and
51 GW200224_222234 [7] both have a Blip glitch identified at Hanford, and a Chirp
52 at Livingston; while GW200129_065458 has a Chirp at both, in addition to a Fast
53 Scattering glitch at Livingston [7]. For GW191109_010717 there are Scattered Light
54 glitches at both detectors, plus a Blip at Livingston [7].

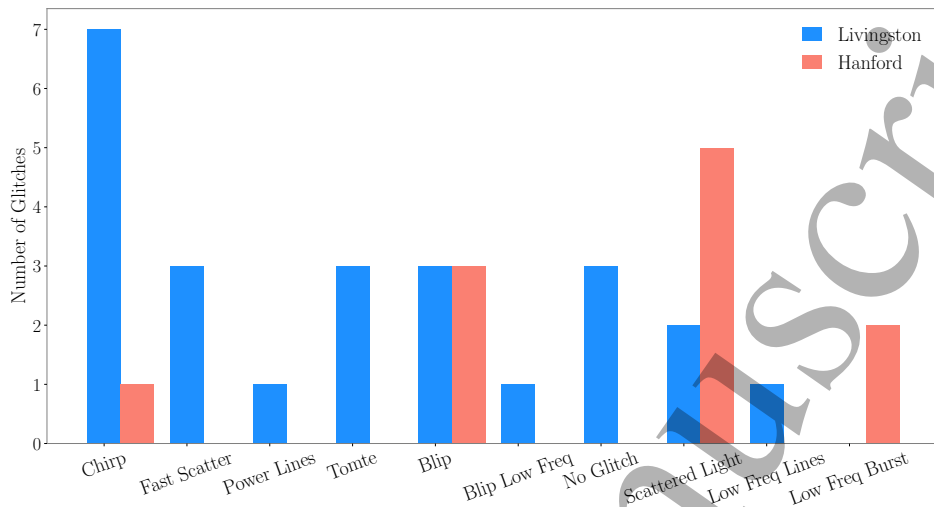
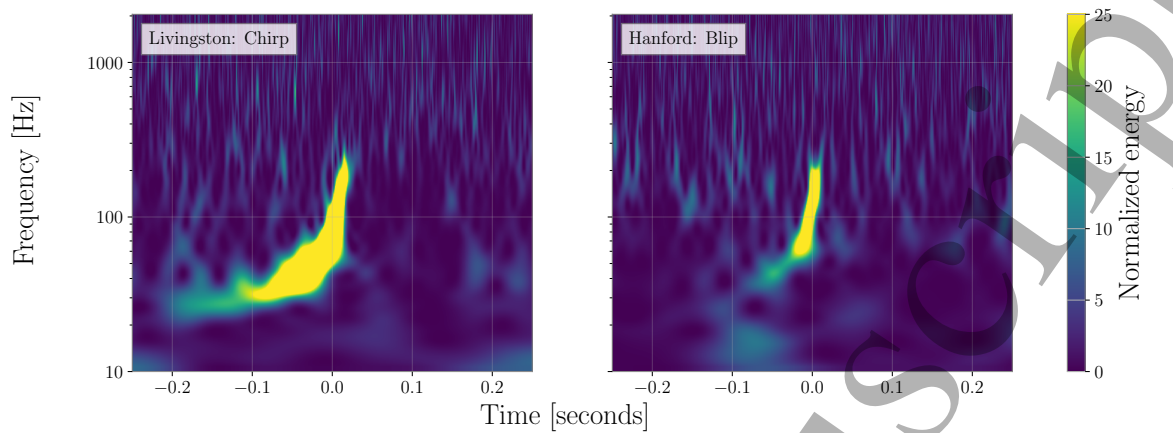
1
2 *Gravity Spy O3 data set*
3
4
5
6
7
8
9
10
11
12
13
14
15
16
17
18
19
20
21
22
23
24
25
26
27
28
29
30
31
32
33
34
35
36
37
38
39
40
41
42
43
44
45
46
47
48
49
50
51
52
53
54
55
56
57
58
59
60

Figure 7: Gravity Spy classifications around O3 gravitational-wave candidates at LIGO Hanford and Livingston. For each candidate, a window of ± 5 s used to identify entries in the Gravity Spy data set. The machine-learning algorithm may be attempting to classify a gravitational-wave signal, a nearby glitch, or some combination of the two; it has not been trained to identify the full diversity of astrophysical gravitational-wave signals, nor how to classify data containing both a signal and a glitch.

The distribution of Gravity Spy classifications is shown in Fig. 7

The Chirp class was originally created for hardware injections (simulated signals used for testing) representing compact binary coalescences [128], and hence might be expected to capture many of these candidates, as is the case. However, a chirp-like time-frequency morphology is only visible for the highest SNR signals; as Livingston is the more sensitive detector, there are more high SNR signals in its data. Tome and Blip share a similar morphology to Chirps, and so may be confused for lower-SNR signals. Figure 8 illustrates an example (GW190521_074359 [5]) where the higher-SNR Livingston signal is classified as a Chirp, while the lower-SNR Hanford signal is (mis)classified as a Blip.

When a candidate is present at the same time as a glitch, it may be that the glitch is picked up by the classification algorithm. Data-quality checks [129] indicated that data mitigation was needed for many candidates from O3 where there was excess noise overlapping the gravitational-wave signal. GW190413_134308, GW190701_203306, GW190814 and GW200129_065458 all required data mitigation for Livingston data, while GW191109_010717 and GW191127_050227 required data mitigation for Hanford data [5, 7]. These all correspond to cases where there is a Gravity Spy classification of a glitch outside of the Chirp–Blip–Tomte family in the relevant detector. However, there is not a perfect correlation between instances where data mitigation was required and Gravity Spy glitch classifications, and there are both candidates where mitigation

1
2 *Gravity Spy O3 data set*
3
4

19
20 Figure 8: Gravitational-wave candidate GW190521_074359 [5]. At Livingston, this
21 glitch was classified as a Chirp, and at Hanford it was classified as a Blip. The SNR
22 of the signal is higher in Livingston, which is why the chirp-like structure is easier to
23 identify.
24

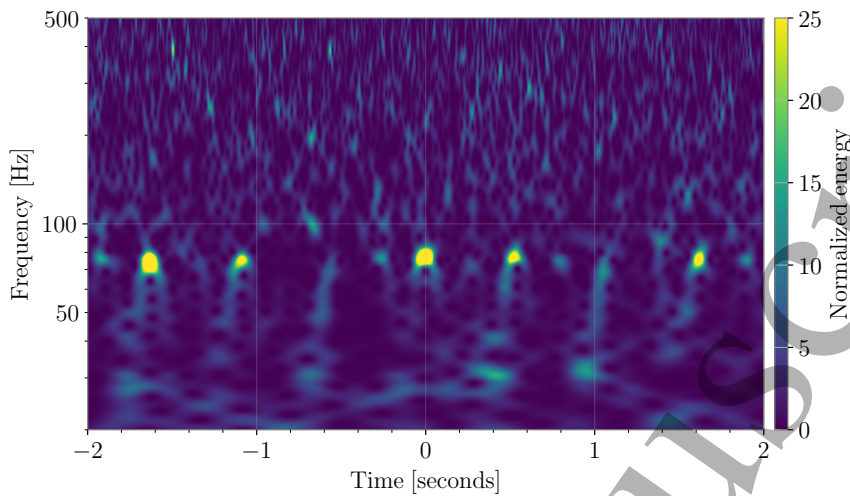
25
26 was required, but there is no entry in the Gravity Spy data set, and candidates where
27 there is a Gravity Spy glitch classification but no data mitigation was required. The
28 former could happen if the excess noise was below the threshold for Omicron trigger, but
29 still identified by the careful data-quality checks performed to evaluate candidates. The
30 latter could happen if the noise is at a frequency that does not impact signal analysis
31 (e.g., $\lesssim 20$ Hz), or if the CNN is confused by the combination of signal plus noise,
32 and makes a misclassification. The Gravity Spy training set does not currently include
33 examples of signals plus glitches.
34

35 To summarise, Gravity Spy is *not* a detection algorithm, but a noise-classification
36 algorithm. As such, it is not intended to discriminate between gravitational-wave
37 signals and glitches. Most gravitational-wave signals are comparatively low in SNR,
38 making them more difficult to be picked up by Gravity Spy. Even when analysed by
39 Gravity Spy, gravitational-wave signals will not all currently be put into the Chirp class.
40 Consequently, the glitch classifications are contaminated (at a low rate) by gravitational-
41 wave signals.
42

43 Along with analyzing the O3 gravitational-wave candidates, we also looked at other
44 candidates that were determined to be false alarms. During these events at Hanford,
45 the most common glitch type seen was Scattered Light. At Livingston, there was more
46 of a variety ranging from Tomtes, Koi Fish, Extremely Loud, Fast Scattering, and No
47 Glitch.
48

49 Of the candidates with an instrumental origin, the glitches classified as No Glitch
50 are of particular interest: for the retracted candidate S190524q, there were 4 glitches
51 classified as No Glitch. Figure 9 shows data around S190524q [5, 103], and despite the
52 No Glitch classification, there is excess power visible. These glitches appear like a high-
53 frequency analogue of Fast Scattering, which does not match any existing Gravity Spy
54

1
2 Gravity Spy O3 data set
3
4
5
6
7
8
9
10
11
12
13
14
15
16
17
18
19
20



21 Figure 9: Example of a Livingston trigger classified as No Glitch from a time
22 corresponding to the retracted candidate S190524q [5, 103]. Despite being labelled as
23 No Glitch, the time-frequency resembles a high-frequency Fast Scattering glitch. This
24 trigger was classified by the Gravity Spy CNN with a confidence of 94%.

25
26
27
28 class. This highlights how the existing set of classes does not catch the full diversity of
29 noise in the detector, and that further refinements of the CNN are needed to properly
30 classify new types of glitches.
31

32 3.3. Data release

33
34 The data release of Gravity Spy machine-learning classifications is available from
35 Zenodo [46]. This consists of comma-separated value (CSV) files for each detector and
36 observing run (O1, O2, O3a and O3b). The CSV files consist of columns describing:
37 (i) metadata output from the Omicron pipeline [26, 27] such as the time of the trigger,
38 trigger peak frequency, bandwidth and amplitude, as well as the data analysed (the
39 main gravitational-wave strain channel); (ii) the unique Gravity Spy identifier of the
40 glitch; (iii) the machine-learning confidence for each of the original 22 glitch categories;
41 (iv) the machine-learning classification and the confidence of this, and (v) links to Omega
42 scans hosted by Zooniverse. Times are given as Global Positioning System (GPS) times,
43 and can be used to identify the relevant data from the Gravitational Wave Open Science
44 Center (GWOSC) [21].⁺ Examples of how to use the data release are given in a Python
45 notebook accompanying the release.
46

47 4. Discussion

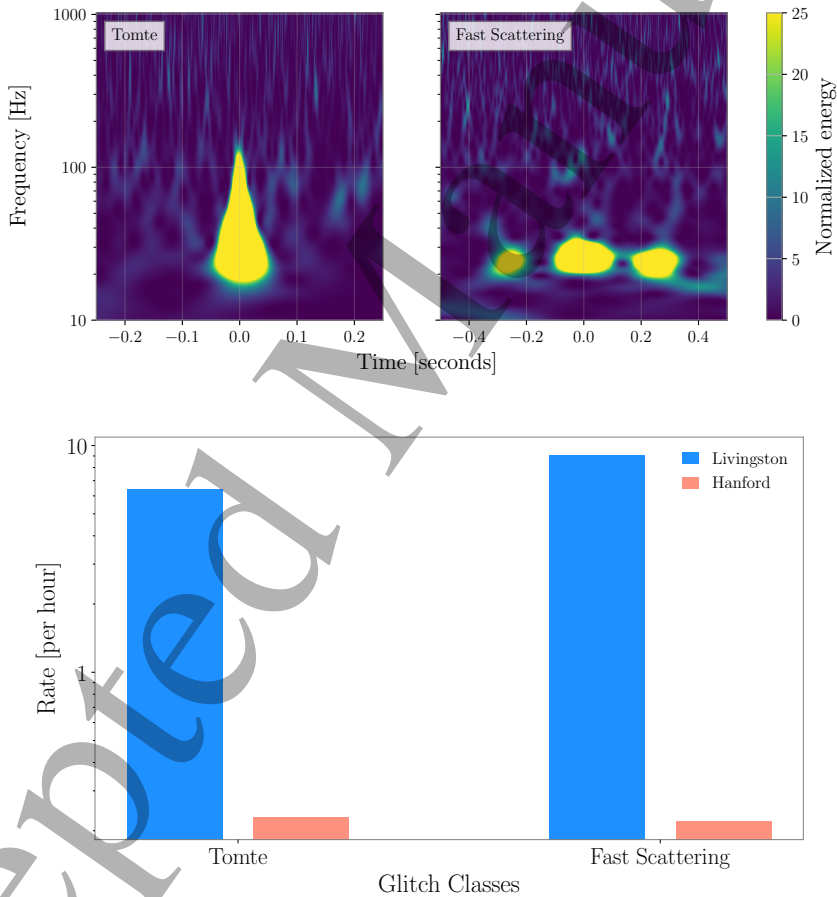
48 The LIGO detectors in Livingston, Louisiana and Hanford, Washington nominally
49 share an identical design [1], and thus we might not expect their performance to
50

51
52
53
54
55
56
57
58
59
60 ⁺ GWOSC gw-openscience.org/

1
2 *Gravity Spy O3 data set*
3
4

19

5 differ much from each other. However, due to differences in their commissioning
 6 progress [74, 77, 78], and in their surrounding environments, the two observatories do
 7 differ in practice [4, 5, 7, 20, 76]. For example, due to the presence of extra low-frequency
 8 noise at Hanford during O3, its sensitivity is about a factor of 2 lower in the frequency
 9 band 20–60 Hz, as compared to Livingston [78]. Additionally, the amount of ground
 10 motion in the anthropogenic (1–6 Hz) and microseism (0.1–0.5 Hz) bands is usually
 11 larger near Livingston than near Hanford. Consequently, there can be considerable
 12 difference in the amount and nature of transient noise between the two detectors: during
 13 O3b, the rate of Omicron transients with SNR above 10 at Livingston was about 1.7
 14 times higher than at Hanford.
 15



49
 50 Figure 10: Time–frequency morphology of the glitch categories Tomte and Fast
 51 Scattering shown in the *top* plot. Both of these classes were more common at Livingston
 52 than at Hanford during O3, as shown in plot on the *bottom*.
 53
 54

55 We see a difference in the number and distribution of glitches across the different
 56 Gravity Spy classes (e.g., Table 1). For example, during O3, the glitch classes Tomte
 57 and Fast Scattering were more common in Livingston, and this increased prevalence
 58 boosted the overall glitch rate [20, 42, 130]. Examples of these two glitches classes, and
 59
 60

1
2 *Gravity Spy O3 data set* 20
34 a comparison of their prevalence during O3 is shown in Fig. 10.
56 Fast Scattering was first noticed as a significant source of noise during the
7 engineering runs preceding O3 [42, 131]. The prevalence of Fast Scattering was a primary
8 motivation for updating the Gravity Spy model to include new classes for the analysis
9 of O3 data [42]. Nearly all Fast Scattering during O3 is below ~ 60 Hz. This transient
10 noise is linked to an increase in ground motion in the anthropogenic and microseism
11 bands near the detector [132, 133]. These two bands are usually noisier at Livingston
12 than at Hanford, and this (combined with the differences in the detectors' low-frequency
13 sensitivity) meant that Fast Scattering was more common at Livingston (9.05 per hour)
14 than at Hanford (0.22 per hour) [20, 134].
1516 Unlike Fast Scattering, we have not yet been able to identify an environmental
17 or instrumental coupling that can explain the origin of Tomte glitches. There are
18 ongoing detector characterisation efforts to understand how this glitch may couple in
19 the detector [130]. While we do not know the origins of Tomte glitches, we do observe
20 a difference in their prevalence at the two observatories: during O3, the rate of Tomte
21 glitches at Livingston was 6.44 per hour, while at Hanford the rate was 0.23 per hour.
22 Tomte glitches have most of their power below ~ 64 Hz. The difference in the low-
23 frequency sensitivity between the two detectors may be partially responsible for the
24 difference in the rates during O3. Further study of when Tomte glitches occur, and the
25 differences between Livingston and Hanford, may reveal the origins of these glitches.
2627 A successful example of detector characterisation during O3 was the identification
28 of the source of Scattered Light (Slow Scattering) glitches, and its subsequent
29 mitigation [56]. Scattered Light glitches have a significant impact on data quality
30 because they occupy a large region time-frequency parameter space. As shown in Fig. 1,
31 Scattered Light transients appear as long-duration arches in spectrograms. These arches
32 are characteristic of noise caused by light scattering. While the frequency gives some
33 information on the motion of the component scattering the light, it is still difficult to
34 identify the troublesome light path in the detectors. The Gravity Spy analysis played
35 a significant role in understanding the source of Scattered Light: the occurrence of
36 glitches classified as Scattered Light was found to correlate with motion of the the
37 quad suspension [20, 56], which is captured by the optical shadow sensors and magnetic
38 actuators (OSEMS) [135, 136], indicating that the source of light scattering was part of
39 the suspension system. The motion was subsequently reduced by employing reaction-
40 chain tracking, which resulted in a considerable reduction in the rate of Scattered Light
41 for the same degree of ground motion near the observatories [56]. The resulting drop
42 in the glitch rate is visible in Fig. 5. This decline in the glitch rate of Scattered Light
43 is sharper at Hanford than at Livingston due comparatively higher ground motion near
44 Livingston in the microseism band during February 2020 [7, 20].
4546 The fourth observing run (O4) will see the use of new and improved
47 technologies [137]. Among them are frequency-dependent squeezing, new Faraday
48 isolators, new test mass mirrors at Livingston, and higher laser power. These
49 improvements will translate to a higher instrument sensitivity, thereby increasing our
50

1
2 *Gravity Spy O3 data set*
3
4

21

5 astrophysical reach for detecting gravitational-wave signals. However, a more sensitive
6 detector is not just more sensitive to gravitational waves, it is also more sensitive to
7 environmental and instrumental noise artifacts. Compared to O2, the rate of glitches
8 during O3a was four times higher at Livingston [5]. Like O3, it is possible that in O4 we
9 will witness one or more new types of noise transients, and that these will appear only
10 at one of the detectors. This could require using a *site-specific* Gravity Spy training
11 set and CNN model to properly characterise O4 data quality. The current plan for O4
12 is to sample the transients for any new glitch morphologies during the engineering run
13 preceding O4, and retrain Gravity Spy before observing starts.

17
18 **5. Summary**
19

20 Understanding data quality is a key aspect of gravitational-wave detector characterisation.
21 The Gravity Spy machine-learning algorithm enables automated classification of
22 segments of LIGO data suspected to contain transient noise. Gravity Spy is routinely
23 used in studies of data quality [20], has been integral in the identification of new classes
24 of glitches [42], and has aided in the identification of the sources of glitches [56]. Here
25 we describe the data release of classifications for O1, O2 and O3. Using CNN models
26 trained for O1–O2 [39, 40] and for O3 [42], we have analysed Advanced LIGO data from
27 these first three observing runs; the results are publicly available from Zenodo [46].
28 These can be used for a range of studies, from investigating environmental and instru-
29 mental origins of glitches, to developing new data-analysis pipelines; we have used the
30 Gravity Spy classifications to illustrate some of the properties of data quality in O3 (as
31 well as highlighting some limitations of the data set).

32 This release covers data from O1–O3. O4 (and subsequent observing runs) [74]
33 will follow improvements to the detector that may lead to the appearance of new glitch
34 classes (and possibly the elimination of current glitch classes). Therefore, the Gravity
35 Spy machine-learning model may need to be updated to account for these changes. To
36 aid detector-characterisation experts in identifying new glitch classes and building a
37 training set of example glitches, we will draw upon the Zooniverse volunteers along with
38 machine-learning clustering approaches. Gravity Spy volunteers have previously rapidly
39 identified new classes based upon their time–frequency morphologies [42], and for O4
40 we will support their investigations into the causes of glitches by providing them with
41 additional auxiliary channel data. Following the update of glitches classes, we anticipate
42 that the classifications provided by the Gravity Spy project will enable further studies
43 of LIGO data quality and improvements to data-analysis pipelines.

54
55 **Acknowledgments**
56

57 We thank the citizen-science volunteers of Gravity Spy who have contributed to the
58 classifications of LIGO data. We are grateful to Marissa Walker and the anonymous
59 referees for comments on the manuscript. Gravity Spy is partly supported by the

1
2 *Gravity Spy O3 data set* 22
3
4

National Science Foundation (NSF) award INSPIRE 1547880 and partially by award IIS-2107334. This work is supported by the NSF under grant PHY-1912648. JG is supported by NSF grant PHY-2110509. SB acknowledges support by NSF grants PHY-1912648 and IIS-2107334. SS acknowledges support of the NSF grant PHY-1764464 to the LIGO Laboratory. MZ is supported by NASA through the NASA Hubble Fellowship grant HST-HF2-51474.001-A awarded by the Space Telescope Science Institute, which is operated by the Association of Universities for Research in Astronomy, Incorporated, under NASA contract NAS5-26555. CPLB acknowledges support from the CIERA Board of Visitors Research Professorship, and Science and Technology Facilities Council (STFC) grant ST/V005634/1. OP is supported by NSF grant PHY-1559694. VK was partially supported through a CIFAR Senior Fellowship, NSF grant PHY-1912648, and by Northwestern University. This material is based upon work supported by NSF's LIGO Laboratory which is a major facility fully funded by the National Science Foundation. This research has made use of data and software obtained from GWOSC (gw-openscience.org), a service of LIGO Laboratory, the LIGO Scientific Collaboration, the Virgo Collaboration, and KAGRA. The authors gratefully acknowledge the support of the United States NSF for the construction and operation of the LIGO Laboratory and Advanced LIGO as well as STFC of the United Kingdom, and the Max-Planck-Society for support of the construction of Advanced LIGO. Additional support for Advanced LIGO was provided by the Australian Research Council. Advanced LIGO was built under award PHY-0823459. LIGO was constructed by the California Institute of Technology and Massachusetts Institute of Technology with funding from the National Science Foundation and operates under Cooperative Agreement PHY-1764464. This work used computing resources at CIERA funded by NSF grant PHY-1726951, and the computational resources and staff contributions provided for the Quest high performance computing facility at Northwestern University which is jointly supported by the Office of the Provost, the Office for Research, and Northwestern University Information Technology. The authors are grateful for computational resources provided by the LIGO Laboratory and supported by National Science Foundation Grants PHY-0757058 and PHY-0823459. This document has been assigned LIGO document number [LIGO-P2200238](#). The data that support the findings of this study are openly available from Zenodo [\[46\]](#).

48
49 **Appendix A. Glitch classes**
50

51 The Gravity Spy projects classifies images into a range of classes. For LIGO data from
52 O1 and O2, 22 classes are used in the CNN model [\[39\]](#) [\[40\]](#), and for data from O3 23
53 classes (the older classes except None of the Above, plus Fast Scattering and Blip Low
54 Frequency) are used [\[42\]](#). In alphabetical order, the set of classes are,:
55

56 (i) *1080 Lines*: These appear as short-duration dots repeating every ~ 0.1 s at
57 ~ 1080 Hz. They are also accompanied by noise below 64 Hz. These glitches were
58 prevalent in Hanford data early in O2, but were reduced following improvements in
59

1
2
3
4
5
6
7
8
9
10
11
12
13
14
15
16
17
18
19
20
21
22
23
24
25
26
27
28
29
30
31
32
33
34
35
36
37
38
39
40
41
42
43
44
45
46
47
48
49
50
51
52
53
54
55
56
57
58
59
60

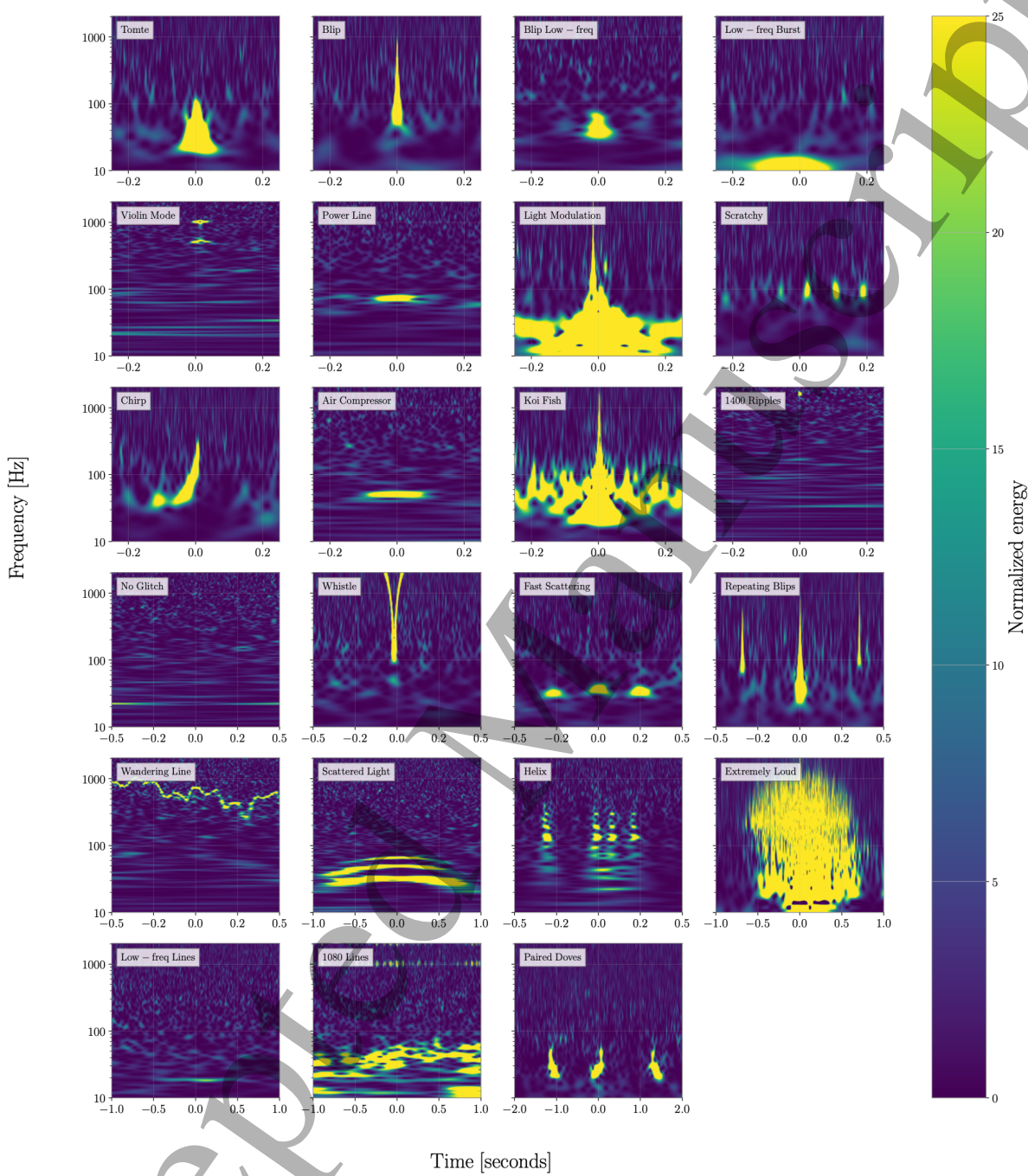
1
2 Gravity Spy O3 data set
3

Figure A1: Time-frequency morphology for examples of the Gravity Spy classes in O3. The classes are grouped by the time duration (0.5 s, 1 s, 2 s or 4 s) that best illustrates their features. *First row*: Tomte, Blip, Blip Low Frequency and Low-frequency Burst (0.5 s). *Second row*: Violin Mode, Power Line, Light Modulation and Scratches (0.5 s). *Third row*: Chirp, Air Compressor, Koi Fish and 1400 Ripples (0.5 s). *Fourth row*: No Glitch, Whistle, Fast Scattering and Repeating Blips (1 s). *Fifth row*: Wandering Line, Scattered Light, Helix (1 s) and Extremely Loud (2 s). *Sixth row*: Low-frequency Lines, 1080 Lines and Paired Doves (4 s). The Blip Low Frequency and Fast Scattering classes are not used for O1 and O2, but the O1 and O2 results do include an additional None of the Above class.

1
2 *Gravity Spy O3 data set*

24

3 the output mode cleaner [138].

4 (ii) *1400 Ripples*: These glitches appear as short ($\lesssim 0.05$ s) wavy lines at ~ 1400 Hz.

5 (iii) *Air Compressor*: This class appears as thick flat line at ~ 50 Hz. In Hanford, these
6 were found to be related to air compressor motors at the end stations [139], and
7 were reduced following the replacement the vibration isolators.

8 (iv) *Blip*: Blip glitches are broadband with very short (~ 0.04 s) duration. Due to
9 their teardrop morphology, Blips can adversely influence the search for high-mass
10 binary black hole signals. Despite being a common glitch class, the cause of Blips
11 is currently unknown [19].

12 (v) *Blip Low Frequency*: Otherwise known as *Low-frequency Blips*, these glitches have
13 a similar morphology to Blip glitches, except they occur at lower frequencies with
14 peak frequencies ~ 10 –50 Hz [42]. This is a new glitch class added for O3.

15 (vi) *Chirp*: The characteristic sweep from low frequencies to high of a coalescing
16 compact-object binary. The class originally contained examples of simulated signals
17 created by hardware injections [128]. The Chirp training set was created early in
18 the era of gravitational-wave astronomy to accommodate hardware injections, and
19 is not representative of our current understanding of the population of coalescing
20 binaries [7, 140].

21 (vii) *Extremely Loud*: These broadband transients are characterised by very high SNR,
22 often leading to the spectrograms appearing saturated. These correspond to large
23 disturbances to the detectors, and may often be accompanied by a drop in the
24 astrophysical range of the detector. High-SNR glitches from other classes (e.g., Koi
25 Fish) may be classified as Extremely Loud.

26 (viii) *Fast Scattering*: Otherwise known as *Crown*, these glitches appear as short-duration
27 (~ 0.2 –0.3 s) arches [42]. These arches often appear in groups, each separated by
28 either 0.25 s or 0.5 s. They are correlated with ground motion in the anthropogenic
29 (1–6 Hz) band, which is usually caused by bad weather or human activity. This is a
30 new glitch class added for O3, and they were the most common glitch in Livingston
31 data.

32 (ix) *Helix*: These are broadband glitches, usually in the frequency region 16–512 Hz,
33 often occurring in groups of two or three glitches separated from each other by
34 ~ 0.1 s. They may be related to glitches in the auxiliary lasers used to calibrate
35 the detectors [139].

36 (x) *Koi Fish*: These glitches are high-SNR broadband glitches. They typically occupy
37 the frequency band ~ 20 –1000 Hz, and can resemble Blips, but with pectoral fins
38 at ~ 30 Hz.

39 (xi) *Light Modulation*: These transients are usually high SNR, with most of the noise
40 content at 16–128 Hz, but there may also be one or more broadband spikes. They
41 are caused by amplitude fluctuations in the control signal of the optical sidebands
42 used to regulate the length and alignment of optical cavities [17].

1
2 *Gravity Spy O3 data set*
3
4

25

5 (xii) *Low-frequency Burst*: These are usually short-duration (~ 0.25 s) transients
6 between ~ 10 – 20 Hz, often appearing as a hump at the bottom of the spectrogram.
7 They were common at Livingston data during O1 and Hanford data in O3a.

8 (xiii) *Low-frequency Lines*: These appear mostly as flat lines, extending ~ 1.5 – 2 s in
9 time and usually below ~ 20 Hz.

10 (xiv) *No Glitch*: This category is used for Omicron triggers where there is not visible
11 excess power in the Gravity Spy spectrogram. These are usually low-SNR Omicron
12 triggers, but can include short-duration, high-frequency ($\gtrsim 2000$ Hz) transients
13 than are difficult to resolve because of the logarithmic frequency scale used for the
14 spectrograms.

15 (xv) *None of the Above*: This category is a catch-all for glitches that do not fit into
16 the other categories. Accordingly, there is no typical morphology. This class is
17 primarily useful when Zooniverse volunteers are classifying images. This class was
18 not used for the final CNN classification of O3 data.

19 (xvi) *Paired Doves*: These appear as a pair of short duration transients, alternating
20 between increasing and decreasing in frequency, with a separation of ~ 0.1 s. These
21 glitches are potentially related to periods of excess motion of the beamsplitter [141].

22 (xvii) *Power Line*: These glitches appear as narrow, flat lines, usually ~ 0.2 – 0.5 s close to
23 60 Hz (or harmonics of this). This frequency corresponds to the electric power-grid
24 frequency in United States, and glitches can be caused by a range of equipment
25 that runs off this power supply [142, 143].

26 (xviii) *Repeating Blips*: This class consists of multiple Blip-like glitches, often repeating
27 with a cadence of ~ 0.25 – 0.50 s.

28 (xix) *Scattered Light*: Otherwise known as *Slow Scattering* (to distinguish from Fast
29 Scattering), they appear as long-duration (~ 2.0 – 2.5 s) arches in the spectrograms.
30 They are correlated with ground motion in the earthquake (0.03– 0.1 Hz) or
31 microseism (0.1– 0.5 Hz) frequency bands. In O3, it was found that Scattered Light
32 was caused by the relative motion between the optical suspension system's end
33 test-mass chain and the reaction-mass chain [56].

34 (xx) *Scratchy*: Sometimes known as *Blue Mountains*, these appear as a series of sharp
35 peaks at intermediate frequencies ~ 60 – 250 Hz. There may be ~ 10 – 30 peaks per
36 second. They are related to light scattering from the Swiss cheese baffles [144, 145].

37 (XXI) *Tomte*: These are short-duration glitches with a characteristic triangular shape.
38 They are similar to Blip or Blip Low-frequency glitches, and typically occupy the
39 frequency band ~ 16 – 150 Hz. They can adversely influence the search for high-mass
40 binary black hole signals.

41 (xxii) *Violin Mode*: These appear as disturbances at ~ 500 Hz and harmonics. These
42 frequencies correspond to the resonances of the glass fibres that are used to suspend
43 the mirrors.

1
2 *REFERENCES* 26
3

4
5 (xxiii) *Wandering Line*: These long-duration transients have an undulating line
6 morphology. They can cover a wide range of frequencies, with multiple lines
7 appearing at once at different frequencies, but are usually above ~ 256 Hz.
8

9 (xxiv) *Whistle*: Also known as *Radio Frequency Beat Notes*, these appear as U-, V- or W-
10 shaped transients, typically above ~ 128 Hz with most of the noise content above
11 ~ 500 Hz. They are caused when radio-frequency signals beat with the voltage
12 controlled oscillators [146].
13

14 Examples for the 23 classes used for O3 classification are shown in Figure A1.
15

16 In addition to the classes used in the CNN, there are additional LIGO glitch classes
17 that have been proposed by Zooniverse volunteers during O3 that have not yet been
18 incorporated into the machine-learning framework:
19

20 (i) *70 Hz Line*: These appear as lines similar to Air Compressor or Power Line glitches,
21 but centred at ~ 70 Hz.
22

23 (ii) *High-frequency Burst*: These appear as very short-duration transients at frequencies
24 $\gtrsim 1000$ Hz.
25

26 (iii) *Pizzicato*: These appear as a short (~ 0.05 s) transient that resembles a flying
27 saucer centered around ~ 500 Hz, ~ 1000 Hz, or both. The frequencies correspond
28 to violin modes of the suspension fibres, and the glitch may be related violin mode
29 damping mechanisms, but the exact cause is yet to be identified.
30

31 These, and further classes, may be added to the CNN for future studies.
32

33
34 *References*

35
36

[1] Aasi J *et al.* (LIGO Scientific Collaboration) 2015 *Class. Quant. Grav.* **32** 074001
37 (*Preprint* [1411.4547](#))
38

[2] Acernese F *et al.* (Virgo Collaboration) 2015 *Class. Quant. Grav.* **32** 024001
39 (*Preprint* [1408.3978](#))
40

[3] Abbott B *et al.* (LIGO Scientific and Virgo Collaboration) 2016 *Phys. Rev. Lett.*
41 **116** 061102 (*Preprint* [1602.03837](#))
42

[4] Abbott B P *et al.* (LIGO Scientific and Virgo Collaboration) 2019 *Phys. Rev. X*
43 **9** 031040 (*Preprint* [1811.12907](#))
44

[5] Abbott R *et al.* (LIGO Scientific and Virgo Collaboration) 2021 *Phys. Rev. X* **11**
45 021053 (*Preprint* [2010.14527](#))
46

[6] Abbott R *et al.* (LIGO Scientific and Virgo Collaboration) 2021 (*Preprint*
47 [2108.01045](#))
48

[7] Abbott R *et al.* (LIGO Scientific, Virgo and KAGRA Collaboration) 2021
49 (*Preprint* [2111.03606](#))
50

[8] Abbott B P *et al.* (LIGO Scientific and Virgo Collaboration) 2016 *Phys. Rev. X*
51 **6** 041015 [Erratum: *Phys. Rev. X* **8** 039903 (2018)] (*Preprint* [1606.04856](#))
52

1
2 *REFERENCES*
3
4

27

[9] Thorne K S 1987 Gravitational radiation *Three Hundred Years of Gravitation* (Cambridge: Cambridge University Press) pp 330–458

[10] Abbott B P *et al.* (LIGO Scientific and Virgo Collaboration) 2020 *Class. Quant. Grav.* **37** 055002 (*Preprint* [1908.11170](https://arxiv.org/abs/1908.11170))

[11] Dal Canton T, Bhagwat S, Dhurandhar S V and Lundgren A 2014 *Class. Quant. Grav.* **31** 015016 (*Preprint* [1304.0008](https://arxiv.org/abs/1304.0008))

[12] Abbott B P *et al.* (LIGO Scientific and Virgo Collaboration) 2018 *Class. Quant. Grav.* **35** 065010 (*Preprint* [1710.02185](https://arxiv.org/abs/1710.02185))

[13] Pankow C *et al.* 2018 *Phys. Rev. D* **98** 084016 (*Preprint* [1808.03619](https://arxiv.org/abs/1808.03619))

[14] Powell J 2018 *Class. Quant. Grav.* **35** 155017 (*Preprint* [1803.11346](https://arxiv.org/abs/1803.11346))

[15] Chatzioannou K, Cornish N, Wijngaarden M and Littenberg T B 2021 *Phys. Rev. D* **103** 044013 (*Preprint* [2101.01200](https://arxiv.org/abs/2101.01200))

[16] Payne E, Hourihane S, Golomb J, Udall R, Davis D and Chatzioannou K 2022 *Phys. Rev. D* **106** 104017 (*Preprint* [2206.11932](https://arxiv.org/abs/2206.11932))

[17] Abbott B *et al.* (LIGO Scientific and Virgo Collaboration) 2016 *Class. Quant. Grav.* **33** 134001 (*Preprint* [1602.03844](https://arxiv.org/abs/1602.03844))

[18] Nuttall L K 2018 *Phil. Trans. Roy. Soc. Lond. A* **376** 20170286 (*Preprint* [1804.07592](https://arxiv.org/abs/1804.07592))

[19] Cabero M *et al.* 2019 *Class. Quant. Grav.* **36** 15 (*Preprint* [1901.05093](https://arxiv.org/abs/1901.05093))

[20] Davis D *et al.* (LIGO Instrument Science Collaboration) 2021 *Class. Quant. Grav.* **38** 135014 (*Preprint* [2101.11673](https://arxiv.org/abs/2101.11673))

[21] Davis D and Walker M 2022 *Galaxies* **10** 12

[22] Akutsu T *et al.* (KAGRA) 2021 *PTEP* **2021** 05A102 (*Preprint* [2009.09305](https://arxiv.org/abs/2009.09305))

[23] Acernese F *et al.* (Virgo Collaboration) 2022 (*Preprint* [2205.01555](https://arxiv.org/abs/2205.01555))

[24] Macleod D, Urban A L, Smith J and Massinger T 2019 gwdetchar/hveto: 1.0.1 URL <https://doi.org/10.5281/zenodo.3532131>

[25] Urban A L, Macleod D, Massinger T, Bidler J, Smith J, Macedo A, Soni S, Coughlin S, Leman K, Davis D and Lundgren A 2019 gwdetchar/gwdetchar: 1.0.2 URL <https://doi.org/10.5281/zenodo.3592169>

[26] Robinet F 2015 Omicron: An Algorithm to Detect and Characterize Transient Noise in Gravitational-Wave Detectors Tech. Rep. VIR-0545C-14 Virgo URL <https://tds.ego-gw.it/ql/?c=10651>

[27] Robinet F, Arnaud N, Leroy N, Lundgren A, Macleod D and McIver J 2020 *SoftwareX* **12** 100620 (*Preprint* [2007.11374](https://arxiv.org/abs/2007.11374))

[28] Cuoco E *et al.* 2021 *Mach. Learn. Sci. Tech.* **2** 011002 (*Preprint* [2005.03745](https://arxiv.org/abs/2005.03745))

[29] Biswas R *et al.* 2013 *Phys. Rev. D* **88** 062003 (*Preprint* [1303.6984](https://arxiv.org/abs/1303.6984))

[30] Tiwari V *et al.* 2015 *Class. Quant. Grav.* **32** 165014 (*Preprint* [1503.07476](https://arxiv.org/abs/1503.07476))

1
2 *REFERENCES*
3
4

28

[31] Mukund N, Abraham S, Kandhasamy S, Mitra S and Philip N S 2017 *Phys. Rev. D* **95** 104059 (*Preprint* [1609.07259](https://arxiv.org/abs/1609.07259))

[32] Cavaglia M, Staats K and Gill T 2019 *Commun. Comput. Phys.* **25** 963–987 (*Preprint* [1812.05225](https://arxiv.org/abs/1812.05225))

[33] Razzano M and Cuoco E 2018 *Class. Quant. Grav.* **35** 095016 (*Preprint* [1803.09933](https://arxiv.org/abs/1803.09933))

[34] Vajente G, Huang Y, Isi M, Driggers J C, Kissel J S, Szczepanczyk M J and Vitale S 2020 *Phys. Rev. D* **101** 042003 (*Preprint* [1911.09083](https://arxiv.org/abs/1911.09083))

[35] Biswas A, McIver J and Mahabal A 2020 *Class. Quant. Grav.* **37** 175008 (*Preprint* [1910.12143](https://arxiv.org/abs/1910.12143))

[36] Colgan R E, Corley K R, Lau Y, Bartos I, Wright J N, Marka Z and Marka S 2020 *Phys. Rev. D* **101** 102003 (*Preprint* [1911.11831](https://arxiv.org/abs/1911.11831))

[37] Essick R, Godwin P, Hanna C, Blackburn L and Katsavounidis E 2020 *Mach. Learn.: Sci. Technol.* **2** 015004 (*Preprint* [2005.12761](https://arxiv.org/abs/2005.12761))

[38] Ormiston R, Nguyen T, Coughlin M, Adhikari R X and Katsavounidis E 2020 *Phys. Rev. Res.* **2** 033066 (*Preprint* [2005.06534](https://arxiv.org/abs/2005.06534))

[39] Zevin M *et al.* 2017 *Class. Quant. Grav.* **34** 064003 (*Preprint* [1611.04596](https://arxiv.org/abs/1611.04596))

[40] Bahaadini S, Noroozi V, Rohani N, Coughlin S, Zevin M, Smith J R, Kalogera V and Katsaggelos A 2018 *Info. Sci.* **444** 172–186

[41] Coughlin S *et al.* 2019 *Phys. Rev. D* **99** 082002 (*Preprint* [1903.04058](https://arxiv.org/abs/1903.04058))

[42] Soni S *et al.* 2021 *Class. Quant. Grav.* **38** 195016 (*Preprint* [2103.12104](https://arxiv.org/abs/2103.12104))

[43] Di Renzo F, Fidecaro F, Hemming G, Katsanevas S and Razzano M 2022 *PoS ICHEP2022* 1152

[44] Bahaadini S, Noroozi V, Rohani N, Coughlin S, Zevin M, Smith J, Kalogera V and Katsaggelos A 2018 Machine learning for Gravity Spy: Glitch classification and dataset URL <https://doi.org/10.5281/zenodo.1476156>

[45] Coughlin S 2018 Updated Gravity Spy Data Set URL <https://doi.org/10.5281/zenodo.1476551>

[46] Coughlin S, Zevin M, Bahaadini S, Rohani N, Allen S, Berry C, Crowston K, Harandi M, Jackson C, Kalogera V, Katsaggelos A, Noroozi V, Osterlund C, Patane O, Smith J, Soni S and Trouille L 2021 Gravity Spy Machine Learning Classifications of LIGO Glitches from Observing Runs O1, O2, O3a, and O3b URL <https://doi.org/10.5281/zenodo.5649212>

[47] Zevin M, Coughlin S, Chase E, Allen S, Bahaadini S, Berry C, Crowston K, Harandi M, Jackson C, Kalogera V, Katsaggelos A, Osterlund C, Patane O, Rohani N, Smith J, Soni S and Trouille L 2022 Gravity Spy Volunteer Classifications of LIGO Glitches from Observing Runs O1, O2, O3a, and O3b URL <https://doi.org/10.5281/zenodo.5911227>

1
2 *REFERENCES*
3
4

29

[48] Davis D, White L V and Saulson P R 2020 *Class. Quant. Grav.* **37** 145001 (*Preprint* [2002.09429](#))

[49] Ashton G, Thiele S, Lecoeuche Y, McIver J and Nuttall L K 2022 *Class. Quant. Grav.* **39** 175004 (*Preprint* [2110.02689](#))

[50] Macas R, Pooley J, Nuttall L K, Davis D, Dyer M J, Lecoeuche Y, Lyman J D, McIver J and Rink K 2022 *Phys. Rev. D* **105** 103021 (*Preprint* [2202.00344](#))

[51] Hourihane S, Chatzioannou K, Wijngaarden M, Davis D, Littenberg T and Cornish N 2022 *Phys. Rev. D* **106** 042006 (*Preprint* [2205.13580](#))

[52] Torres-Forné A, Cuoco E, Font J A and Marquina A 2020 *Phys. Rev. D* **102** 023011 (*Preprint* [2002.11668](#))

[53] Merritt J, Farr B, Hur R, Edelman B and Doctor Z 2021 *Phys. Rev. D* **104** 102004 (*Preprint* [2108.12044](#))

[54] Lopez M, Boudart V, Buijsman K, Reza A and Caudill S 2022 *Phys. Rev. D* **106** 023027 (*Preprint* [2203.06494](#))

[55] Powell J, Sun L, Gereb K, Lasky P D and Dollmann M 2022 (*Preprint* [2207.00207](#))

[56] Soni S *et al.* (LIGO Instrument Science Collaboration) 2020 *Class. Quant. Grav.* **38** 025016 (*Preprint* [2007.14876](#))

[57] Longo A, Bianchi S, Valdes G, Arnaud N and Plastino W 2022 *Class. Quant. Grav.* **39** 035001 (*Preprint* [2112.06046](#))

[58] Colgan R E, Márka Z, Yan J, Bartos I, Wright J N and Márka S 2022 (*Preprint* [2203.05086](#))

[59] Benkő Z, Bábé T and Somogyvári Z 2022 *Sci. Rep.* **12** 227 (*Preprint* [2004.11468](#))

[60] Marianer T, Poznanski D and Prochaska J X 2020 *Mon. Not. Roy. Astron. Soc.* **500** 5408–5419 (*Preprint* [2010.11949](#))

[61] Jadhav S, Mukund N, Gadre B, Mitra S and Abraham S 2021 *Phys. Rev. D* **104** 064051 (*Preprint* [2010.08584](#))

[62] Singh S, Singh A, Prajapati A and Pathak K N 2021 *Mon. Not. Roy. Astron. Soc.* **508** 1358–1370 (*Preprint* [2008.06550](#))

[63] Abbott T C, Buffaz E, Vieira N, Cabero M, Haggard D, Mahabal A and McIver J 2022 *Astrophys. J.* **927** 232 (*Preprint* [2111.04015](#))

[64] Chaturvedi P, Khan A, Tian M, Huerta E A and Zheng H 2022 *Front. Artif. Intell.* **5** 828672 (*Preprint* [2201.11133](#))

[65] Choudhary S, More A, Suyamprakasam S and Bose S 2022 (*Preprint* [2202.08671](#))

[66] George D, Shen H and Huerta E A 2017 (*Preprint* [1706.07446](#))

[67] Sankarapandian S and Kulis B 2021 (*Preprint* [2107.10667](#))

[68] Sakai Y *et al.* 2022 *Sci. Rep.* **12** 9935 (*Preprint* [2111.10053](#))

[69] Yan J, Leung A P and Hui D C Y 2022 *Mon. Not. Roy. Astron. Soc.* **515** 4606–4621 (*Preprint* [2207.04001](#))

1
2 *REFERENCES*
3
4

5 [70] Akutsu T *et al.* (KAGRA Collaboration) 2019 *Nature Astron.* **3** 35–40 (*Preprint*
6 [1811.08079](#))

7 [71] Abbott R *et al.* (LIGO Scientific and Virgo Collaboration) 2021 *SoftwareX* **13**
8 100658 (*Preprint* [1912.11716](#))

9 [72] Nguyen P *et al.* (LIGO Instrument Science Collaboration) 2021 *Class. Quant.
10 Grav.* **38** 145001 (*Preprint* [2101.09935](#))

11 [73] Acernese F *et al.* (Virgo Collaboration) 2022 (*Preprint* [2203.04014](#))

12 [74] Abbott B *et al.* (KAGRA, LIGO Scientific and Virgo Collaboration) 2020 *Living
13 Rel. Rel.* **23** 3 (*Preprint* [1304.0670](#))

14 [75] Abbott B P *et al.* (LIGO Scientific and Virgo Collaboration) 2016 *Phys. Rev. Lett.*
15 **116** 131103 (*Preprint* [1602.03838](#))

16 [76] Martynov D V *et al.* (LIGO Instrument Science Collaboration) 2016 *Phys. Rev. D*
17 **93** 112004 [Addendum: *Phys. Rev. D* **97** 059901 (2018)] (*Preprint* [1604.00439](#))

18 [77] Abbott B P *et al.* (LIGO Scientific and Virgo Collaboration) 2017 *Phys. Rev. Lett.*
19 **118** 221101 [Erratum: *Phys. Rev. Lett.* **121** 129901 (2018)] (*Preprint* [1706.01812](#))

20 [78] Buikema A *et al.* (LIGO Instrument Science Collaboration) 2020 *Phys. Rev. D*
21 **102** 062003 (*Preprint* [2008.01301](#))

22 [79] Covas P B *et al.* (LIGO Instrument Science Collaboration) 2018 *Phys. Rev. D* **97**
23 082002 (*Preprint* [1801.07204](#))

24 [80] Chatterji S, Blackburn L, Martin G and Katsavounidis E 2004 *Class. Quant. Grav.*
25 **21** S1809–S1818 (*Preprint* [gr-qc/0412119](#))

26 [81] Soni S 2020 aLIGO LLO Logbook [52071](#)

27 [82] Accadia T *et al.* 2010 *Class. Quant. Grav.* **27** 194011

28 [83] Valdes G, O'Reilly B and Diaz M 2017 *Class. Quant. Grav.* **34** 235009

29 [84] Bahaadini S, Rohani N, Coughlin S, Zevin M, Kalogera V and Katsaggelos A K
30 2017 Deep Multi-view Models for Glitch Classification *2017 IEEE International
31 Conference on Acoustics, Speech and Signal Processing (ICASSP)* pp 2931–2935
32 (*Preprint* [1705.00034](#))

33 [85] Ottaway D J, Fritschel P and Waldman S J 2012 *Opt. Express* **20**

34 [86] Chen H Y, Holz D E, Miller J, Evans M, Vitale S and Creighton J 2021 *Class.
35 Quant. Grav.* **38** 055010 (*Preprint* [1709.08079](#))

36 [87] Abbott R *et al.* (LIGO Scientific, Virgo and KAGRA Collaboration) 2022 *Astron.
37 Astrophys.* **659** A84 (*Preprint* [2105.15120](#))

38 [88] Abbott R *et al.* (LIGO Scientific, Virgo and KAGRA Collaboration) 2021
39 (*Preprint* [2107.03701](#))

40 [89] Abbott R *et al.* (LIGO Scientific, Virgo and KAGRA Collaboration) 2021 *Phys.
41 Rev. D* **104** 102001 (*Preprint* [2107.13796](#))

42 [90] Mishra T *et al.* 2022 *Phys. Rev. D* **105** 083018 (*Preprint* [2201.01495](#))

1
2 *REFERENCES*
3
4

31

[91] Olsen S, Venumadhav T, Mushkin J, Roulet J, Zackay B and Zaldarriaga M 2022 *Phys. Rev. D* **106** 043009 (*Preprint* [2201.02252](https://arxiv.org/abs/2201.02252))

[92] Nitz A H, Kumar S, Wang Y F, Kastha S, Wu S, Schäfer M, Dhurkunde R and Capano C D 2021 (*Preprint* [2112.06878](https://arxiv.org/abs/2112.06878))

[93] LIGO Scientific and Virgo Collaboration 2019 *GCN* **25870** URL <https://gcn.gsfc.nasa.gov/other/S190930s.gcn3>

[94] LIGO Scientific and Virgo Collaboration 2019 *GCN* **25883** URL <https://gcn.gsfc.nasa.gov/other/S190928c.gcn3>

[95] LIGO Scientific and Virgo Collaboration 2019 *GCN* **25828** URL <https://gcn.gsfc.nasa.gov/other/S190924h.gcn3>

[96] LIGO Scientific and Virgo Collaboration 2019 *GCN* **25554** URL <https://gcn.gsfc.nasa.gov/other/S190829u.gcn3>

[97] LIGO Scientific and Virgo Collaboration 2019 *GCN* **25320** URL <https://gcn.gsfc.nasa.gov/other/S190814bv.gcn3>

[98] Abbott R *et al.* (LIGO Scientific and Virgo Collaboration) 2020 *Astrophys. J. Lett.* **896** L44 (*Preprint* [2006.12611](https://arxiv.org/abs/2006.12611))

[99] LIGO Scientific and Virgo Collaboration 2019 *GCN* **25295** URL <https://gcn.gsfc.nasa.gov/other/S190808ae.gcn3>

[100] LIGO Scientific and Virgo Collaboration 2019 *GCN* **25183** URL <https://gcn.gsfc.nasa.gov/other/S190728q.gcn3>

[101] LIGO Scientific and Virgo Collaboration 2019 *GCN* **24948** URL <https://gcn.gsfc.nasa.gov/other/S190701ah.gcn3>

[102] LIGO Scientific and Virgo Collaboration 2019 *GCN* **24920** URL <https://gcn.gsfc.nasa.gov/other/S1906030ag.gcn3>

[103] LIGO Scientific and Virgo Collaboration 2019 *GCN* **24655** URL <https://gcn.gsfc.nasa.gov/other/S190524q.gcn3>

[104] LIGO Scientific and Virgo Collaboration 2019 *GCN* **24629** URL <https://gcn.gsfc.nasa.gov/other/S190521r.gcn3>

[105] LIGO Scientific and Virgo Collaboration 2019 *GCN* **24618** URL <https://gcn.gsfc.nasa.gov/other/S190521g.gcn3>

[106] Abbott R *et al.* (LIGO Scientific and Virgo Collaboration) 2020 *Phys. Rev. Lett.* **125** 101102 (*Preprint* [2009.01075](https://arxiv.org/abs/2009.01075))

[107] LIGO Scientific and Virgo Collaboration 2019 *GCN* **24598** URL <https://gcn.gsfc.nasa.gov/other/S190519bj.gcn3>

[108] LIGO Scientific and Virgo Collaboration 2019 *GCN* **24503** URL <https://gcn.gsfc.nasa.gov/other/S190512at.gcn3>

[109] LIGO Scientific and Virgo Collaboration 2019 *GCN* **24141** URL <https://gcn.gsfc.nasa.gov/other/S190421ar.gcn3>

1
2 *REFERENCES* 32
3

4

5 [110] LIGO Scientific and Virgo Collaboration 2019 *GCN* **24098** URL <https://gcn.gsfc.nasa.gov/other/S190412m.gcn3>

6

7 [111] Abbott R *et al.* (LIGO Scientific and Virgo Collaboration) 2020 *Phys. Rev. D* **102** 8
9 043015 (*Preprint* [2004.08342](https://arxiv.org/abs/2004.08342))

10

11 [112] LIGO Scientific and Virgo Collaboration 2019 *GCN* **24063** URL <https://gcn.gsfc.nasa.gov/other/S190408an.gcn3>

12

13 [113] LIGO Scientific and Virgo Collaboration 2020 *GCN* **27358** URL <https://gcn.gsfc.nasa.gov/other/S200311bg.gcn3>

14

15 [114] LIGO Scientific and Virgo Collaboration 2020 *GCN* **27184** URL <https://gcn.gsfc.nasa.gov/other/S200224ca.gcn3>

16

17 [115] LIGO Scientific and Virgo Collaboration 2020 *GCN* **26926** URL <https://gcn.gsfc.nasa.gov/other/S200129m.gcn3>

18

19 [116] LIGO Scientific and Virgo Collaboration 2020 *GCN* **26785** URL <https://gcn.gsfc.nasa.gov/other/S200116ah.gcn3>

20

21 [117] LIGO Scientific and Virgo Collaboration 2020 *GCN* **26734** URL <https://gcn.gsfc.nasa.gov/other/S200114f.gcn3>

22

23 [118] LIGO Scientific and Virgo Collaboration 2020 *GCN* **26715** URL <https://gcn.gsfc.nasa.gov/other/S200112r.gcn3>

24

25 [119] LIGO Scientific and Virgo Collaboration 2020 *GCN* **26665** URL <https://gcn.gsfc.nasa.gov/other/S200108v.gcn3>

26

27 [120] LIGO Scientific and Virgo Collaboration 2020 *GCN* **26641** URL <https://gcn.gsfc.nasa.gov/other/S200106au.gcn3>

28

29 [121] LIGO Scientific and Virgo Collaboration 2019 *GCN* **26585** URL <https://gcn.gsfc.nasa.gov/other/S191225aq.gcn3>

30

31 [122] LIGO Scientific and Virgo Collaboration 2019 *GCN* **26402** URL <https://gcn.gsfc.nasa.gov/other/S191213g.gcn3>

32

33 [123] LIGO Scientific and Virgo Collaboration 2019 *GCN* **26394** URL <https://gcn.gsfc.nasa.gov/other/S191212q.gcn3>

34

35 [124] LIGO Scientific and Virgo Collaboration 2019 *GCN* **26263** URL <https://gcn.gsfc.nasa.gov/other/S191120aj.gcn3>

36

37 [125] LIGO Scientific and Virgo Collaboration 2019 *GCN* **26254** URL <https://gcn.gsfc.nasa.gov/other/S191117j.gcn3>

38

39 [126] LIGO Scientific and Virgo Collaboration 2019 *GCN* **26218** URL <https://gcn.gsfc.nasa.gov/other/S191110x.gcn3>

40

41 [127] LIGO Scientific and Virgo Collaboration 2019 *GCN* **26202** URL <https://gcn.gsfc.nasa.gov/other/S191109d.gcn3>

42

43 [128] Biwer C *et al.* 2017 *Phys. Rev. D* **95** 062002 (*Preprint* [1612.07864](https://arxiv.org/abs/1612.07864))

44

45 [129] Davis D, Littenberg T B, Romero-Shaw I M, Millhouse M, McIver J, Di Renzo F
46 and Ashton G 2022 *Class. Quant. Grav.* **39** 245013 (*Preprint* [2207.03429](https://arxiv.org/abs/2207.03429))

47

48

49

50

51

52

53

54

55

56

57

58

59

60

1
2 *REFERENCES*
3

4
5 [130] Soni S 2021 aLIGO LLO Logbook 54936
6 [131] Smith J 2019 aLIGO LLO Logbook 44803
7 [132] Soni S, Effler A, Frolov V and Schofield R 2020 Fast scattering noise at LIGO and
8 DetChar Noise sprint Tech. Rep. G2001639 LSC URL <https://dcc.ligo.org/LIGO-G2001639/public>
9
10 [133] Soni S, Effler A, Glanzer J and Frolov V 2021 Fast Scattering Corner Station
11 Coupling at LLO Tech. Rep. G2102369 LSC URL <https://dcc.ligo.org/LIGO-G2102369>
12
13 [134] Patron A 2020 aLIGO LLO Logbook 53678
14
15 [135] Aston S M *et al.* 2012 *Class. Quant. Grav.* **29** 235004
16
17 [136] Matichard F *et al.* 2015 *Class. Quant. Grav.* **32** 185003 (*Preprint* 1502.06300)
18
19 [137] Cahillane C and Mansell G 2022 *Galaxies* **10** 36 (*Preprint* 2202.00847)
20
21 [138] Dwyer S 2017 aLIGO LHO Logbook 33104
22
23 [139] Smith J 2015 aLIGO LLO Logbook 21436
24
25 [140] Abbott R *et al.* (LIGO Scientific, Virgo and KAGRA Collaboration) 2021
26
27 (*Preprint* 2111.03634)
28
29 [141] Lundgren A 2016 aLIGO LHO Logbook 27138
30
31 [142] Sorazu B 2015 aLIGO LHO Logbook 23483
32
33 [143] Smith J 2017 aLIGO LLO Logbook 32389
34
35 [144] Schofield R 2017 aLIGO LHO Logbook 36147
36
37 [145] Patane O 2018 aLIGO LHO Logbook 43177
38
39 [146] Nuttall L *et al.* 2015 *Class. Quant. Grav.* **32** 245005 (*Preprint* 1508.07316)
40
41
42
43
44
45
46
47
48
49
50
51
52
53
54
55
56
57
58
59
60